Peripheral opioid receptor antagonism alleviates fentanyl-induced cardiorespiratory depression and is devoid of aversive effects

[1,2,3]Brian C. Ruyle, [1,2,3]Sarah Masud, [1,2,3]Rohith Kesaraju, [1,2,3]Mubariz Tahirkheli, [1,2,3]Juhi Modh, [1,2,3]Sofia Angulo-Lopera, [1,2,3]Tania Lintz, [1,2,3]Jessica A. Higginbotham, [1,2,3]Nicolas Massaly, [1,2,3,4,5]Jose A Moron*

Affiliations:

[1]Department of Anesthesiology, Washington University in St Louis; St. Louis, MO, USA

[2]Pain Center, Washington University in St Louis; St. Louis, MO, USA

[3]School of Medicine, Washington University in St. Louis; St. Louis, MO, USA

[4]Department of Neuroscience, Washington University in St. Louis; St. Louis, MO, USA

[5]Department of Psychiatry, Washington University in St. Louis; St. Louis, MO, USA

*corresponding author Email: jmoron-concepcion@wustl.edu

ABSTRACT

Millions of Americans suffering from Opioid Use Disorders (OUD) face a high risk of fatal overdose due to opioid-induced respiratory depression (OIRD). Fentanyl, a powerful synthetic opioid, is a major contributor to the rising rates of overdose deaths. Reversing fentanyl-induced respiratory depression has proved to be challenging due to both its high potency and lipophilicity. We assessed the contributions of central and peripheral mu opioid receptors (MORs) in mediating fentanyl-induced physiological responses. The peripherally-restricted MOR antagonist naloxone methiodide (NLXM) both prevented and reversed OIRD to a comparable extent as naloxone (NLX), indicating substantial involvement of peripheral MORs to OIRD. Interestingly, NLXM-mediated OIRD reversal did not produce aversive behaviors observed after NLX. We show that neurons in the nucleus of the solitary tract (nTS), the first central synapse of peripheral afferents, exhibit biphasic patterns of activity following fentanyl exposure. NLXM pretreatment attenuates this activity, suggesting that these responses are mediated by peripheral MORs. Together, these findings establish a critical role for peripheral MOR, including ascending inputs to the nTS, as sites of dysfunction during OIRD. Furthermore, selective peripheral MOR antagonism could be a promising therapeutic strategy for managing OIRD by sparing CNS-driven acute opioid-associated withdrawal and aversion observed after NLX.

Keywords

Opioids, brainstem, respiratory depression, opioid receptors, fentanyl

Significance Statement:

In this study, we compare the central versus peripheral components underlying fentanyl-induced cardiorespiratory depression to prevent overdose deaths. Our data indicates that these effects are, at least partially, due to the activation of mu opioid receptors present in peripheral sites. These findings provide insight into peripheral contributions to fentanyl-induced overdoses and could potentially lead to the development of treatments selectively targeting the peripheral system, sparing individuals from the CNS-driven acute opioid withdrawal generally observed with the use of naloxone.

INTRODUCTION

Millions of Americans live with Opioid Use Disorders (OUD) and face a high risk of opioid-induced respiratory depression (OIRD), the leading cause of opioid related deaths (*1*). The number of fatalities attributed to OIRD has been exacerbated by the rise of distribution and use of synthetic opioids, such as fentanyl (*2*–*5*). Fentanyl is a highly lipophilic opioid that readily crosses the blood-brain barrier and binds tightly to mu opioid receptors (MORs), which are abundant in the respiratory centers of the medulla and pons (*1*, *6*, *7*). Compared to other opioids such as heroin and morphine, fentanyl exhibits both a faster onset of OIRD and higher potency for MOR binding (*8*, *9*), minimizing successful prevention of lethal outcomes using naloxone (NLX), a competitive and preferential MOR antagonist (*10*, *11*). Despite its high efficacy in reversing OIRD, NLX also precipitates unpleasant withdrawal symptoms and aversion, as reported in patients and preclinical models (*11*–*13*), making its implementation for managing OUD challenging. Therefore, a better understanding of the pharmacology, specific brain regions and pathways, and physiological responses induced by high doses of fentanyl are necessary to develop effective prevention and intervention strategies, ultimately saving lives of patients suffering from OUD.

Several regions have been implicated as key sites of triggering OIRD, including the Pre-Botzinger Complex in the brainstem and the parabrachial nucleus and Kolliker-Fuse nucleus in the pons (*1*, *14*–*19*). Opioids act directly within these networks to alter inspiratory and expiratory phase duration, leading to overall reductions in respiratory rate (*17*, *20*). In addition, the nucleus of the solitary tract (nTS), located in the dorsal brainstem, is the first central site that receives sensory afferent information via cranial nerves related to cardiorespiratory, gustatory and gastrointestinal function (*21*). Acute hypoxia robustly activates nTS neurons (*22*, *23*) to initiate

65 appropriate autonomic and cardiorespiratory responses that facilitate a return to homeostatic
66 physiological states. MOR is highly expressed in the nTS, primarily on vagal afferent fibers that
67 terminate within the nTS(*24*). Interestingly, opioids induce systemic and brain hypoxia (*25*, *26*)
68 and produce an increase in Fos-immunoreactivity in the nTS (*27*, *28*). However, engaging MOR
69 signaling in the nTS impairs hypoxic ventilatory responses (*7*), suggesting that OIRD may result
70 from nTS dysfunction failing to engage appropriate cardiorespiratory responses, leading to
71 prolonged OIRD. However, the specific contributions of nTS MOR, including ascending MOR-
72 expressing inputs to this region, in driving aberrant cardiorespiratory depression are still not fully
73 understood.
74 In addition to their high expression throughout brainstem respiratory nuclei, MORs are also
75 expressed in the periphery, including sensory ganglia, lung afferents, cardiac tissue and cranial
76 nerves that terminate within the nTS (*29*, *30*). Naloxone Methiodide (NLXM) is a quaternary
77 derivative of NLX that does not cross the blood brain barrier at low doses, making it a useful tool
78 to assess the peripheral vs central contribution of MORs in opioid-induced physiology and
79 behavior (*10*, *31*). Despite its lower binding affinity for MOR, NLXM has been shown to reverse
80 opioid-induced hypoventilation and brain hypoxia in rodent models (*12*, *31*, *32*), suggesting that
81 peripheral opioid receptors may play a greater role in OIRD than previously thought. However,
82 no studies to date have provided a comprehensive assessment of opioid-induced
83 cardiorespiratory depression and systemic hypoxia combined with a real-time assessment of
84 MOR-mediated activity of nTS neurons.
85 In the present study, we examined the relative contributions of central and peripheral MORs
86 mediating fentanyl-induced depression of cardiorespiratory parameters and investigated
87 potential mechanisms of opioid-induced dysfunction within the nTS. We report that fentanyl-
88 induced cardiorespiratory depression and prolonged systemic hypoxia can be prevented or
89 reversed by NLXM to a degree similar to NLX. As compared to NLX, NLXM-mediated reversal
90 of OIRD does not produce aversive-like behaviors. Fentanyl induced robust Fos-IR expression
91 in the nTS in a dose-dependent manner, and this activation can be attributed to a combination
92 of direct effects of opioids acting at MOR located within the nTS and the subsequent hypoxia
93 that develops after fentanyl exposure. Given that the majority of nTS MOR is located on vagal
94 afferent fibers, we utilized various techniques to evaluate opioid-induced activity within the nTS
95 and manipulate nTS MOR signaling during OIRD. Using wireless *in vivo* fiber photometry, we
96 show that fentanyl induces a biphasic pattern of activity in nTS, characterized by a transient
97 increase followed by a prolonged decrease in neuronal excitability. NLXM pretreatment strongly
98 attenuated this biphasic response, indicating that fentanyl-induced nTS activity is influenced by

99 MOR-expressing peripheral afferents. Together, these findings provide novel insights into
100 peripheral mechanisms mediating OIRD and support peripheral MOR antagonism as a
101 promising therapeutic strategy for managing OIRD for patients suffering from OUD while sparing
102 the CNS-driven acute aversive behaviors that are observed with the use of NLX.
103

104 RESULTS

105 Intravenous fentanyl induces respiratory depression and activates nTS neurons in a 106 dose-dependent manner

107 We first examined the effect of intravenous fentanyl to induce cardiorespiratory depression and
108 activate neurons in the nucleus tractus solitarius (nTS). Catheterized rats received intravenous
109 saline (1 ml/kg) or fentanyl at a range of doses (2, 20, or 50 µg/kg; **Figure 1A**), and
110 cardiorespiratory parameters were measured up to 60 minutes. The first 20 minutes of these
111 responses are shown in **Figure 1B-D**. Neither saline nor 2 µg/kg fentanyl evoked a significant
112 change in cardiorespiratory parameters. In comparison, both 20 and 50 µg/kg fentanyl produced
113 rapid decreases in oxygen saturation, heart rate, and respiratory rate, with the largest decrease
114 occurring after 50 µg/kg fentanyl. The nadir (defined as the lowest point measured after
115 fentanyl) and recovery (calculated as 90% of baseline values prior to fentanyl) for each
116 physiological parameter were assessed in all groups (**Figure 1E-J**). There was no significant
117 difference in the nadir or recovery values between saline- and 2 µg/kg fentanyl-treated rats. In
118 comparison, rats given 50 µg/kg fentanyl exhibited a significantly lower nadir in oxygen
119 saturation (**Figure 1B,E**) and respiratory rate compared to 20 µg/kg (**Figure 1D,I**). In addition,
120 the recovery time was significantly longer in rats that received 50 µg/kg fentanyl compared to 20
121 µg/kg fentanyl (**Figure 1B,E, D,I)**. The nadir of bradycardia was similar between 20- and 50
122 µg/kg rats (**Figure 1G**), although the duration of the response was significantly longer in rats
123 that received the highest dose of fentanyl (**Figure 1H**). We next examined nTS activation (Fos-
124 IR) following intravenous fentanyl (**Figure 1K)**. A significant increase in Fos-IR was observed
125 after 2 µg/kg fentanyl, (**Figure 1L**), a dose that did not induce OIRD. Further dose-dependent
126 increases in Fos-IR were observed after 20 and 50 µg/kg fentanyl. We evaluated a
127 subpopulation of catecholaminergic nTS neurons, which are critical for full expression of
128 hypoxia-evoked cardiorespiratory responses (*22*, *33*) for activation after intravenous fentanyl
129 (**Figure 1M**). These cells were similarly activated at 2 and 20 µg/kg fentanyl, with a further
130 increase observed at the highest dose (50 µg/kg).
131

132 **Peripheral opioid receptor antagonism prevents fentanyl-induced respiratory depression**

133 The above data provide a comprehensive assessment of the dose-dependent changes
134 in cardiorespiratory parameters and nTS neuronal activation evoked by intravenous fentanyl. To
135 gain insight into the extent to which central and peripheral opioid receptors contribute to these
136 effects, a separate cohort of rats received intravenous administration of the non-selective opioid
137 receptor antagonist naloxone (NLX; 1 mg/kg) or the peripherally-restricted opioid receptor
138 antagonist naloxone methiodide (NLXM, 1 and 5 mg/kg) prior to intravenous fentanyl
139 administration at 20 µg/kg (**Figure 2A**) or 50 µg/kg (**Figure S2A**). It has been previously shown
140 that NLXM does not cross the blood brain barrier at low doses (*31*, *34*). Our data are in
141 agreement with these reports, as we show that neither dose of NLXM reached a significant level
142 within the central nervous system at either time point evaluated (**Figure 6**). Thus, we utilized
143 NLXM to further investigate the roles of peripheral and central MOR in OIRD.

144 As shown in **Figure 2B-D**, saline pretreatment followed by 20 µg/kg fentanyl produced
145 an onset and duration of cardiorespiratory depression similar to **Figure 1**. Similar responses
146 were observed in rats that received saline pretreatment followed by 50 µg/kg fentanyl (**Figure**
147 **S1B-D**). As expected, NLX pretreatment completely blocked the decrease in cardiorespiratory
148 parameters at both 20 µg/kg and 50 µg/kg doses of fentanyl. In rats that received 20 µg/kg
149 fentanyl, 1 mg/kg NLXM pretreatment prevented the bradycardic and hypoventilatory responses
150 to fentanyl (**Figure 21-D**). For all parameters, saline-pretreated rats exhibited lower nadir values
151 than NLX- and NLXM-pretreated rats, and there was no significant difference in the nadir or
152 duration between NLX (1mg/kg) and NLXM (1mg/kg) pretreated rats that received 20 µg/kg
153 fentanyl (**Figure 2E-J**). There was a slight decrease in the nadir of oxygen saturation in NLXM-
154 pretreated rats vs NLX-pretreated rats, although this was not significant (**Figure 2E**, p=0.0876).
155 In rats that received 50 µg/kg fentanyl, 1 mg/kg NLXM pretreatment was unable to prevent the
156 initial decrease in all cardiorespiratory parameters (**Fig S1E,G,I**). However, the duration of these
157 responses was significantly shorter compared to saline-treated rats (**Figure S1F,H,J**). A higher
158 dose of NLXM (5 mg/kg), which does not cross the blood brain barrier (**Figure 5D**), was then
159 used in a separate group of animals that received 50 µg/kg fentanyl. Pretreatment with 5 mg/kg
160 NLXM fully prevented fentanyl-induced bradycardia and hypoventilation but did not completely
161 prevent a decrease in oxygen saturation, although the recovery time was similar to the NLX-
162 pretreated group (p = 0.7151) (**Figure S1B-J**). Together, these data demonstrate that peripheral
163 MOR antagonism is sufficient to prevent 20 µg/kg fentanyl-induced cardiorespiratory depression
164 and strongly attenuates OIRD evoked by 50 µg/kg fentanyl.

165 Neuronal activation, as measured by Fos-IR, was examined in the nTS of rats pretreated
166 with saline or opioid receptor antagonists followed by 20 µg/kg (**Figure 2K**) or 50 µg/kg fentanyl
167 (**Figure S1K**). For fentanyl doses, saline pretreatment evoked the highest degree of Fos-IR in
168 the nTS, including in a subpopulation of TH-IR neurons. Blocking peripheral MOR signaling with
169 NLXM did not decrease fentanyl-induced nTS neuronal activation, while NLX, which blocks both
170 central and peripheral MORs resulted in a significant reduction in nTS activation (**Figure 2L,M**).
171 In rats that received the highest dose of fentanyl, the number of Fos-IR was similar between rats
172 pretreated with saline and NLXM at both doses, with the only significant reduction occurring in
173 NLX-pretreated animals (**Figure S1L**). This pattern of activation was also observed in
174 catecholaminergic cells (**Figure S1M**), although around 30% of TH-IR neurons also displayed
175 Fos-IR in NLX-pretreated rats.
176

177 **Peripheral opioid receptor antagonism reverses fentanyl-induced respiratory depression**

178 The above data demonstrate that peripheral MOR antagonism largely prevents fentanyl-induced
179 respiratory depression but only minimally reduces nTS neuronal activation. Given that reversal
180 of OIRD has more relevance as a therapeutic intervention, we next evaluated the extent to
181 which NLXM reverses cardiorespiratory depression after it has been induced by 20 µg/kg
182 (**Figure 3A**) and 50 µg/kg fentanyl (**Figure S2A**). Both 20 and 50 µg/kg fentanyl induced rapid
183 decreases in oxygen saturation, heart rate and respiratory rate, similar to what was observed in
184 Figure 1 (**Figure 3B-D; Figure S2B-D**). The fentanyl-induced nadir in all physiological
185 parameters was similar prior to intravenous administration of saline, NLX or NLXM. In rats that
186 received 20 µg/kg fentanyl, both intravenous NLX (1 mg/kg) and NLXM (1 mg/kg) quickly
187 restored cardiorespiratory values to baseline significantly faster than saline-pretreated animals
188 (**Figure 3F,H,J**). This reversal of cardiorespiratory parameters was similar between NLX- and
189 NLXM-treated animals. In rats that received 50 µg/kg fentanyl, NLX quickly restored all
190 physiological parameters to their baseline values (**Figure S2F,H,J**). While 1 mg/kg NLXM did
191 not sufficiently reverse the OIRD induced by 50 µg/kg fentanyl (**Figure S2F**)**,** a higher dose of 5
192 mg/kg NLXM fully reversed the fentanyl-induced bradycardia and hypoventilation, similar to
193 NLX. Importantly, this dose of NLXM is not detectable in the central nervous system (**Figure**
194 **5D**). Thus, blocking peripheral MORs is sufficient to fully reverse OIRD.
195 Because acute hypoxia activates nTS neurons (*23*), we investigated the impact of
196 peripheral and central MOR antagonism on fentanyl-induced nTS neuronal activation (**Figure**
197 **3K**). At both doses of fentanyl administered, a similar degree of nTS neuronal activation was
198 observed in all groups regardless of MOR antagonist administered after fentanyl (**Figure 3L,M;**

199 **Figure S2L,M**). Together, these data demonstrate that selective antagonism of peripheral
200 opioid receptors is sufficient to reverse cardiorespiratory depression induced by both moderate
201 and high doses of fentanyl. Moreover, these data suggest that even a brief period of fentanyl-
202 induced cardiorespiratory depression is sufficient to induce robust activation of nTS neurons,
203 and this subsequent MOR antagonism has no additional effect on nTS activation.
204
205 **Reversal of Fentanyl-Induced Respiratory Depression with NLXM is not aversive**
206 NLX rapidly reverses OIRD, but produces unwanted side effects including the immediate
207 onset of severe withdrawal (*12*, *13*). The intense symptoms induced during NLX-precipitated
208 withdrawal present additional challenges in managing OUD in patients. Given that peripheral
209 MOR antagonism sufficiently reverses fentanyl-induced cardiorespiratory depression to a
210 degree that is similar to NLX, we then used a conditioned place aversion (CPA) approach to
211 assess whether selective peripheral antagonism of MOR signaling also mediates aversive
212 behaviors. Rats underwent a 3-session CPA challenge that consisted of a Pre-Conditioning test,
213 Conditioning test, and Post-Conditioning test (**Figure 4A**). Horizontal locomotion in both
214 compartments of the CPA boxes was assessed during both pre- and post-conditioning tests
215 (**Figure 4B**). During the pre-conditioning test, rats exhibited no natural preference or aversion
216 for either compartment. On the Conditioning day (Day 2), a divider was placed in the middle of
217 the CPA box. Rats received intravenous fentanyl injection (50 μg/kg) in their home cage. Four
218 minutes later, rats were placed into the paired compartment of the CPA box and immediately
219 given intravenous saline (1 m1/kg), NLX (1 mg/kg) or NLXM (1 or 5 mg/kg). During the Post-
220 conditioning test, the divider was removed and rats were allowed to explore both compartments
221 of the CPA box. **Figure 4C** shows the time spent on the conditioned side of the CPA box for all
222 groups. During the Post-Conditioning test, NLX-treated animals spent significantly less time in
223 the NLX-paired compartment, highlighting the aversive responses that are evoked by NLX
224 infused after fentanyl treatment. In contrast, NLXM did not produce aversive behaviors to the
225 NLXM-paired compartment, but rather induced a preference at the higher dose (**Figure 4D**), an
226 effect that may be mediated by fentanyl acting at central MORs. Importantly, a single
227 conditioning session with fentanyl administered in the home cage followed by saline in the
228 compartment instead of a MOR antagonist did not produce a preference or aversion to the
229 saline-paired compartment. As shown in **Figure S3**, neither NLX nor NLXM significantly alters
230 physiological parameters from baseline values. To rule out any potential effects of endogenous
231 opioids influencing the behavioral responses to opioid receptor antagonism, we performed an
232 additional test in which rats were given saline in their home cage, followed by NLX or NLXM in

one of the CPA compartments (**Figure 4E,F**). Neither antagonist produced a preference nor aversion to the MOR antagonist-paired compartment (**Figure 4G**). There was no difference in CPA scores between these groups (**Figure 4H**).

Fentanyl induces a biphasic pattern of activity in nTS neurons

As shown in Figure 1, fentanyl induced robust Fos-IR expression in the nTS. While Fos-IR quantification provides insight into the anatomical activation of brainstem subregions in response to fentanyl administration and OIRD reversal, this approach does not provide any temporal resolution of the activity of these cells. Therefore, we used wireless *in vivo* fiber photometry to assess dynamic changes in nTS calcium transient activity after intravenous fentanyl administration in anesthetized rats (**Figure 5A**). Catheterized rats underwent bilateral injections of an AAV expressing a calcium sensor (pGP-AAV-syn-jGCaMP8m-WPRE) into the nTS. On the day of the experiment, an optic fiber was lowered on the surface of the brainstem above the nTS and calcium transient activity was recorded (**Figure 5B**). GCaMP viral expression was observed throughout the caudal-rostral extent of the nTS in all rats (**Figure 5C**). Fentanyl (20 µg/kg) infusion induced a biphasic pattern of activity in the nTS, characterized by an initial robust increase in activity (Early Response) followed by a decrease below baseline (Late Response, **Figure 5D**). Pretreatment with NLXM (5 mg/kg) attenuated both phases of the fentanyl-induced changes in neuronal activity. As shown in **Figure 5E**, the area under the cure (AUC) was significantly elevated during the Early and Late Responses after fentanyl. In contrast, no significant fentanyl-induced change in AUC was observed in NLXM-pretreated rats at either time point, indicating that changes in fentanyl-induced nTS neuronal activity are strongly mediated by peripheral MORs. We next examined the extent to which MOR antagonists restore the fentanyl-induced reductions in activity. After MOR antagonist administration, fentanyl-induced suppression of nTS activity returned to baseline during the early recovery in rats that received NLX, but not NLXM. However, both NLX and NLXM enhanced nTS activity above baseline during the late recovery period (**Figure 5F,G).** During the Late Recovery period, nTS activity was significantly enhanced above baseline in both NLX and NLXM-treated animals. Together, these data demonstrate that peripheral MOR antagonism is sufficient to reverse the fentanyl-induced decrease in nTS neuronal activity.

DISCUSSION

OIRD is a complex problem that continues to be at the forefront of the opioid epidemic (*1*, *35*). The increased potency and faster onset of synthetic opioids like fentanyl has been attributed to the rising wave of opioid-related deaths in the US (*2*, *11*). Numerous studies have

evaluated opioid-induced dysfunction within key regulatory sites in the central nervous system that contribute to the severity of OIRD (*1*, *14*, *15*, *17*, *27*). Peripheral MORs have also been examined for their roles in impacting OIRD (*12*, *32*). However, the specific contributions of central and peripheral MORs to the onset and duration of fentanyl-induced cardiorespiratory depression, along with the role of the nTS in these effects, are not completely understood. In this study, we show that blocking peripheral MORs sufficiently prevents and reverses fentanyl-induced cardiorespiratory depression and systemic hypoxia. Furthermore, we demonstrate that peripheral opioid receptors mediate fentanyl-induced activity of nTS neurons. These data suggest that the nTS may be an area impacted by fentanyl via peripheral MOR activation. Lastly, we demonstrate that in addition to reversing fentanyl-induced cardiorespiratory depression, NLXM does not induce aversive behaviors, as compared to NLX. Together, these findings provide evidence that peripheral MOR antagonism may be a potential novel target to reverse OIRD without inducing withdrawal, anxiety, and aversion, all of which can contribute to further relapse in drug-seeking behaviors (*2*, *13*).

While numerous studies have focused on evaluating the effects of opioids acting at MORs present within brainstem and pontine networks, less attention has been given to identifying peripheral MOR mechanisms contributing to OIRD. NLX is the most common reversal agent used to treat OIRD (*13*, *35*). Despite its efficacy in treating OIRD, NLX induces withdrawal symptoms and aversion in both patients and preclinical models (*12*, *13*, *36*). In this study, we demonstrate that NLX-induced reversal of fentanyl-induced respiratory depression, as shown by a significant decrease in time spent in the NLX-associated compartment. This is likely the result of the induction of withdrawal symptoms that occur following antagonism of MOR in central reward pathways (*12*, *13*, *37*). In contrast, this aversive response was not observed in rats that received NLXM; NLXM-treated rats exhibited a preference for the associated compartment. These data suggest that alleviating fentanyl-induced respiratory distress without antagonizing central MOR may mitigate the aversive state produced by NLX. While previous reports have shown that NLX can be detected centrally after a subcutaneous injection of NLXM (*31*), we report here that no detectable amount of NLX or NLXM was found in brain tissue at the doses used in these studies (1 and 5 mg/kg, intravenous). Similar to NLX, peripheral MOR antagonism with NLXM partially reverses opioid-induced analgesia (*12*, *38*) which may pose limitations for pain management. Future investigations are needed to evaluate mechanisms underlying the therapeutic potential of NLXM as an intervention for managing OIRD in patients with OUDs.

300 The nTS is a region with a high degree of MOR expression, and appears to be primarily
301 located on afferent fibers arising from the vagus nerve (*7*, *24*, *41*). While MOR has been shown
302 to be present in nTS somas and dendrites (*24*, *27*), these MOR-expressing cells do not express
303 Fos following exposure to opioids or hypoxia (*27*), which suggests a mechanism of presynaptic
304 action of MOR signaling in the nTS. Likewise, the nodose ganglion (NG), which contains the cell
305 bodies of nTS-projecting vagal sensory afferents, has high expression of MOR (*30*), and intra-
306 nodose injection of fentanyl induces hypoventilation, although to a much lesser degree
307 compared to systemic fentanyl (*42*).
308 In the present study, we used fiber photometry to characterize nTS neuronal responses
309 to show that fentanyl induces an initial excitatory response in nTS cells. However, this response
310 was short-lasting compared to the subsequent decrease in activity below baseline, suggesting
311 that the primary effect of MOR signaling produce generalized inhibition of nTS neurons. This
312 prolonged suppression of nTS neuronal activity may contribute to the overall duration of OIRD.
313 Furthermore, our photometry data demonstrate that while the NLXM-mediated reversal of
314 fentanyl-induced inhibition of nTS neurons was slower compared to NLX, activity was eventually
315 restored. A similar finding was observed in OIRD experiments, as NLXM induced a rate of
316 recovery in all parameters that was comparable to NLX. Taken together, this suggests that
317 peripheral MOR antagonism may sufficiently override simultaneous central effects of fentanyl
318 acting at MOR present in cardiorespiratory nuclei, including the nTS.
319 It is important to note that while all our experiments assessing fentanyl-induced
320 cardiorespiratory depression were conducted in conscious rats breathing room air, photometry
321 experiments were performed under isoflurane anesthesia. Due to the location of the nTS,
322 chronic fiber implantation and subsequent in vivo photometry recordings in conscious,
323 unrestrained animals is not possible. In the nTS, Isoflurane has been reported to suppress
324 visceral afferent glutamatergic transmission and enhance GABAergic transmission via
325 postsynaptic mechanisms (*39*), as well as induce cFos expression in the nTS (*40*). Precautions
326 were taken to use the lowest dose of isoflurane needed to maintain sufficient anesthesia.
327 However, we cannot rule out the possible influence of isoflurane anesthesia to influence the
328 observed biphasic responses evoked by fentanyl. Nevertheless, our data support a mechanism
329 by which fentanyl induces OIRD via disruption of visceral afferent signaling to the nTS, thereby
330 leading to prolonged OIRD due to suppression of physiological reflex responses that would be
331 normally engaged in response to systemic hypoxia.
332 The nTS plays an essential role in the regulation of basal-and reflex-evoked
333 cardiorespiratory function (*21*). Activation of MOR in the nTS has been shown to blunt hypoxic

334 ventilatory responses following MOR agonism in the nTS (*7*). Our data are consistent with
335 previous work demonstrating opioid-induced activation of nTS neurons (*27*). The degree of
336 fentanyl induced Fos-IR in the nTS resembles what is observed after acute exposure to hypoxic
337 air (20, 46). Interestingly, we also observed increased Fos in the nTS at a dose of fentanyl that
338 was below the threshold to induce respiratory depression. It is unclear whether the Fos-IR
339 observed after low or high doses of fentanyl is, in part, the result of increased glutamatergic
340 transmission stemming from enhanced chemoreceptor afferent signaling to the nTS or via MOR
341 signaling within the nTS itself.

342 Glutamate is the primary neurotransmitter released from sensory afferent fibers into the
343 nTS (*21*, *43*). While intra-nTS application of opioid agonists have been shown to reduce
344 glutamate release and calcium channels via presynaptic mechanisms (*44*, *45*), opioids also
345 have been shown to induce a similar biphasic action of Ca2+-dependent spikes in the nodose
346 ganglion (*46*) that resembles what we observed in GCaMP-expressing nTS cells after
347 intravenous fentanyl. NLXM strongly attenuated the fentanyl-induced excitatory wave observed
348 in GCaMP-expressing nTS neurons, suggesting that MOR-expressing peripheral afferents
349 mediate this transient activation of nTS neurons, even if the primary effect of fentanyl is to inhibit
350 the nTS and suppress cardiorespiratory reflex function.
351 One possibility is that the increase in nTS activity may be mediated by opioid-induced
352 disinhibition within the nTS. The nTS contains a large population of second order GABAergic
353 interneurons that receive direct inputs from visceral afferents (*47*), and hypoxia activates these
354 cells(*22*). nTS MOR agonists suppress the activity of these cells, primarily via presynaptic
355 mechanisms (*48*), although postsynaptic mechanisms have been reported (*49*). Similarly,
356 visceral afferents also activate catecholaminergic nTS neurons (*50*), which are critical for the
357 generation of hypoxia-evoked cardiorespiratory responses(*33*, *51*). Opioids inhibit visceral
358 afferent transmission to this cell group, primarily via a presynaptic mechanism (*44*). In the
359 present study, we observed robust Fos expression in these cells at all doses of fentanyl
360 examined. These findings raise the possibility that nTS dysfunction, via MOR-expressing
361 peripheral inputs that terminate within this region, represents the first central site of fentanyl-
362 induced dysfunction, ultimately leading to downstream effects in other brain regions that
363 contribute to diminished autonomic and cardiorespiratory responses that contribute to the
364 duration of OIRD. Future studies are needed to fully evaluate the exact opioid-MOR effects in
365 the nTS, including specific MOR afferent inputs and the nTS phenotypes, to determine their
366 relative contributions to OIRD.

367 In summary, these studies highlight a significant involvement of peripheral MORs
368 contribute to the rapid cardiorespiratory depression induced by intravenous fentanyl. We have
369 provided extensive characterization into how fentanyl elicits cardiorespiratory depression and
370 examined the relationship between peripheral MORs and nTS activity in contributing to the
371 duration of OIRD. Moreover, our findings suggest that selectively blocking peripheral ORs could
372 be a promising therapeutic strategy for managing OIRD. Notably, peripheral opioid receptor
373 antagonists are already prescribed for patients undergoing chemotherapy to alleviate side
374 effects such as opioid-induced constipation (*52*, *53*). Importantly, our data demonstrate that
375 peripheral MOR antagonism prevents and reverses OIRD without triggering unwanted effects of
376 withdrawal that occur following NLX administration, suggesting that peripheral MOR antagonists
377 like NLXM could potentially be utilized in treatment strategies for managing OUD.

378 Materials and Methods:

379 All surgical and experimental procedures were approved by Washington University Committee
380 in accordance with the National Institutes of Health Guidelines for the Care and Use of
381 Laboratory Animals and Animal Research: Reporting In Vivo Experiments (ARRIVE) guidelines.
382 Rats were initially group-housed with two to three animals per cage on a 12/12-h dark/light cycle
383 (lights on at 7:00) and acclimated to the animal facility holding rooms for at least 7 days before
384 any manipulation. Following catheterization surgery, rats were single-housed and remained on
385 an identical 12/12-h dark/light cycle. The temperature for the holding rooms of all animals
386 ranged from 21 to 24 °C while the humidity was between 30 and 70%. Rats received food and
387 water ad libitum for the duration of all experiments. All experiments were performed during the
388 light cycle. For all experiments, male and female Sprague Dawley rats (250-350g) were used. In
389 all data sets, male rats are represented by filled symbols and female rats are represented by
390 open symbols.

391 **IV catheterization procedure:**

392 Animals were deeply anesthetized using Isoflurane (3% induction, 2% maintenance). A small
393 incision was made in the dorsal surface of the neck. Another small incision was made on the
394 ventral surface of the neck, and underlying tissue was carefully dissected to expose the jugular
395 vein. An indwelling catheter was inserted into the jugular vein and sutured in place using non-
396 absorbable silk suture. The catheter was then tunneled subcutaneously and exited the body
397 through the first small hole in neck on the dorsal side. The ventral incision was closed using
398 non-absorbable silk suture. The exposed catheter was connected to a backpack device
399 (Instech) containing a port for drug administration. Animals were given Carprofen (2 mg/kg sc),
400 Baytril (8 mg/kg sc) and bupivacaine (5 mg/kg, site of incision). In addition, rats were given

401 Carprofen tablets (Bio Serv, MD150-2) for 2 days after surgery to assist in wound healing and
402 analgesia. Rats were singly housed following surgery, and were allowed to recover for one
403 week prior to the commencement of experiments. Catheter patency was maintained with daily
404 flushing of 0.3 mL sterile saline containing gentamicin (1.33 mg/mL, i.v.)

405 **Respiratory depression experiments:**

406 Following recovery from IV catheterization surgery, conscious, freely-moving rats in their home
407 cages were fitted with a non-invasive pulse oximeter collar (Starr LifeSciences).
408 Cardiorespiratory parameters (oxygen saturation, heart rate and respiratory rate) were collected
409 (MouseOx v2.0, Starr LifeSciences) at baseline conditions in animals breathing room air, and
410 after intravenous administration of fentanyl citrate (2, 20 or 50 µg/kg). A subset of animals
411 received weight-adjusted intravenous administration of the nonselective opioid receptor
412 antagonist naloxone hydrochloride (NLX; 1 mg/kg; Sigma 51481-60-8) or the peripherally-
413 restricted opioid receptor antagonist naloxone methiodide (NLXM; 1 or 5 mg/kg; Sigma N129)
414 before or after fentanyl administration. Cardiorespiratory parameters were then measured for up
415 to 60 minutes. For all OIRD experiments, the time course graphs consist of 30 seconds of data
416 averaged into a single data point. The nadir was defined as the lowest point measured after
417 fentanyl administration (for all graphs, red arrow indicates time of fentanyl administration,
418 time=0 minutes). In addition, the recovery rate was defined as the time to reach 90% baseline of
419 pre-fentanyl values for each cardiorespiratory parameter. Two hours after fentanyl
420 administration, rats were transcardially perfused with 0.01M PBS followed by paraformaldehyde
421 (4% in 0.01M PBS). Brains were removed and stored overnight at 4 °C in 4% paraformaldehyde
422 for post-fixation, followed by at least 72 h incubation in sucrose (30% in 0.01M PBS) solution.
423 Isopentane was used to flash-freeze brains. Brainstem sections containing the nTS were sliced
424 in the coronal plane (40 µm) using a cryostat (Leica CM 1950).

425 **Biodistribution**

426 A subset of previously catheterized drug-naïve rats was deeply anesthetized and then received
427 intravenous administration of NLX (1 mg/kg) or NLXM (1 or 5 mg/kg). While still under
428 anesthesia, rats were quickly decapitated two or ten minutes after intravenous administration of
429 MOR antagonists. MOR antagonists were dosed in all rats at an experimentally relevant
430 concentration with triplicate blood and brain samples collected at two time points. The early time
431 point at 2 minutes evaluated conditions when the plasma concentration of the OR antagonist is
432 high and reflects the identical time point of intravenous administration for OIRD pretreatment
433 experiments. The second collection time point (10 minutes) was intended to evaluate steady-
434 state conditions and represent physiological experiments when reversal of OIRD was achieved

435 by both antagonists. Brains were quickly removed and flash frozen in liquid nitrogen. Trunk
436 blood was collected into capillary collection tubes containing lithium heparin (Greiner Bio-One;
437 Fisher Scientific). The blood was spun on a centrifuge for 10 min at 4 °C, and plasma was
438 carefully extracted from the supernatant. Brains and plasma samples underwent PK analyses
439 for detection of NLX or NLXM at both time points. Standard rat PK studies dosed the candidate
440 MOR antagonists and sample blood over multiple time points. A general description of tissue
441 distribution can be obtained during PK modeling by calculating the volume of distribution.
442 Samples underwent a direct measurement of peripheral restriction by measuring compound
443 concentration in plasma and brain.

444 **Conditioned Place Aversion**

445 The aversive effects following reversal of OIRD were measured using Conditioned Place
446 Aversion (CPA) (*54*). During a pre-conditioning session (Day 1), rats were allowed to explore
447 both sides of a two compartment CPA box for 15 minutes. On the Conditioning Day (Day 2), a
448 divider was placed in the middle of the box to restrict movement to one side on the box. Rats
449 were then randomly assigned to one side of the CPA box, and this side was paired with either
450 saline (1 ml/kg), NLX (1 mg/kg) or NLXM (1 or 5 mg/kg). Rats were given intravenous fentanyl
451 (50 μg/kg) or saline in their home cages. Four minutes later, they were placed in the paired side
452 of the box and immediately given saline or a MOR antagonist. Rats were confined to this
453 compartment for 15 minutes. For all CPA experiments, measures were taken to balance the
454 side of CPA box by drug and by sex. On the post-conditioning test (Day 3), the divider was
455 removed. Rats were then placed in the CPA box and allowed to explore both sides of the CPA
456 box for 15 minutes. The total time spent in the paired chamber and CPA scores were calculated
457 for all groups.

458 **In vivo Fiber Photometry**

459 To selectively measure nTS neuronal calcium transient activity, we injected an AAV containing a
460 calcium sensor expressed under the synapsin promoter (pGP-AAV-syn-jGCaMP8m-WPRE) into
461 the nTS (500 nl per side; 0.3-0.5 mm anterior, ± 0.4 mm lateral and 0.4 mm ventral to brain
462 surface, relative to calamus scriptorius). Rats were allowed at least 3 weeks to recover from
463 nanoinjection surgery to allow for robust viral expression in the nTS before IV catheters were
464 implanted as described above. On the day of the experiment, rats were deeply anesthetized
465 with isoflurane (3-4% induction, 2% maintenance), placed in the stereotaxic apparatus, and the
466 nTS was exposed as described above. To overcome limitations associated with chronic fiber
467 implants in the nTS, a wireless photometry headstage (TeleFipho, Amuza Inc.) was secured to
468 a 5 mm flat-tipped silica optic fiber cannula (400 μm c.d./470 μm o.d., NA 0.37, 2.5 mm

469 receptacle; Doric) and mounted the stereotaxic arm with an apparatus 3D printed in house to
470 permit simultaneous nTS exposure and photometry recordings. The optic fiber was lowered to
471 the site of the dorsal brainstem and firmly pressed on the surface above the nTS until a signal
472 was detected (~0.3-0.5 mm ventral from the surface). An LED generated blue light was
473 bandpass-filtered (445-490 nm) to excite jGCaMP8m and emission fluorescence was detected
474 by an internal photodiode detector for green light (bandpass filtered at 500-550 nm). An internal
475 DC amplifier transmitted the data (16-bit arbitrary unit; AU) to a wireless receiver (TeleFipho,
476 Amuza Inc.) and the data was extracted in real-time using TeleFipho software (Amuza Inc.) at a
477 sampling rate of 100 Hz. The offset was set to 90° and the LED power was adjusted to achieve
478 an optimal signal output (30-40k a.u.) not to exceed 36 mW power, and remained constant
479 throughout the recording. Baseline activity of GCaMP fluorescence nTS-infected cells was
480 measured after at least 5 min to mitigate effects of baseline drift in signal due to slow
481 photobleaching artifacts. Then, baseline activity was measured for at least 30 s prior to
482 administration of either fentanyl (20 µg/kg, i.v.) or NLXM (5 mg/kg, i.v.). After response activity
483 was recorded, rats received a second intravenous injection of either an opioid receptor
484 antagonist (NLX,1 mg/kg or NLXM, 5 mg/kg) or fentanyl (20 µg/kg), respectively. Each
485 intravenous administration was manually time locked to calcium transient recordings by a
486 second experimenter and response activity following each injection was recorded for 60 s
487 before administration of the second injection or conclusion of the experiment. Rats were
488 transcardially perfused with PFA at the end of the experiment as described above and viral
489 expression was validated for all animals.
490 For analysis of calcium transient activity, the raw data was fit to a double-exponential curve and
491 subtracted from the raw data to account for any residual effects of baseline drift. Matlab Signal
492 Analyzer was used to extract regions of interest (ROIs) in the signal in 90-s traces (30 s pre-
493 treatment, 60 s post-treatment) and traces were aligned to the time of injection. ROIs were
494 standardized as z-scores using the sample standard deviation, *S,* where $S = \sqrt{\frac{\Sigma_{i=1}^{n}(x_i - \bar{X})^2}{n-1}}$ such
495 that signals were centered to have a mean of 0 and scaled to have a standard deviation of 1.
496 Based on this, the area under the curve (AUC) of ROI z-scores were calculated in 30-s bins
497 using the trapezoidal rule (*trapz* function in Matlab) and one-sample t-tests were used to
498 determine differences relative to baseline (theoretical mean = 0). For presentation, transients
499 were down sampled by a factor of 10 with a phase offset of 2 and the resultant 10 Hz traces
500 were smoothed using a moving mean duration of 5% of total ROI.
501

502 **Immunohistochemistry (IHC):**

503 Immunohistochemical procedures were performed as previously described (*55*). Brainstem
504 sections containing the nTS were sliced using a cryostat (Leica) at a thickness of 40 um. Free-
505 floating sections were rinsed in 0.01M PBS, blocked in 10% Normal Donkey Serum (Sigma) in
506 0.01M PBS-triton, and then incubated with the following antibodies: cFos (Rabbit anti-cFos;
507 ab190289, Abcam; AB_2737414); Tyrosine Hydroxylase (TH, Mouse anti-TH; MAB318,
508 Millipore; AB_2201528). The following day, sections were rinsed with 0.01M PBS, incubated
509 with Donkey anti-Rabbit Cy3 and Donkey anti-Mouse Alexa fluor 488 (1:200; in 3% NDS and
510 0.3% Triton in 0.01M PBS) and used to visualize targets of interest (Jackson ImmunoResearch).

511 **Image acquisition:**

512 Immunoreactivity (IR) and viral expression were examined with a Leica DMR microscope at 20X
513 magnification. 20 µm thick z-stacks of the nTS (2 µm per plane) were collected. ImageJ (v. 1.48,
514 NIH) software was used for post-processing and analysis. In all groups, three sections of the
515 nTS (corresponding to -360, 0, +360 µm relative to calamus scriptorius) were collected.

516 **Brainstem immunohistochemical analyses**

517 Using ImageJ software, the regions containing the nTS were outlined, and unilateral counts of
518 Fos-IR, TH-IR and co-labeled Fos- and TH-IR neurons were performed using a custom-made
519 plugin (Cell Counter) for each of the 3 nTS sections per animal. The total number of each
520 phenotype was summed from these 3 sections.

521 **Statistics**

522 For all experiments, the normality of sample data was determined using D'Agostino and
523 Pearson tests and Shapiro–Wilk tests. Statistical significance was taken as * $p<0.05$, ** $p<0.01$,
524 *** $p<0.001$ and ****$p<0.0001$, as determined by two-way repeated measures analysis of
525 variance (ANOVA) followed by Sidak's post hoc test; one-way ANOVA with Tukey post-hoc test,
526 two-tailed unpaired t-test, two-tailed paired t-test, one sample t-test.

527

528

529

530

531

532

533

534 ## References

535 1. J.-M. Ramirez, N. J. Burgraff, A. D. Wei, N. A. Baertsch, A. G. Varga, H. A. Baghdoyan, R.
536 Lydic, K. F. Morris, D. C. Bolser, E. S. Levitt, Neuronal mechanisms underlying opioid-
537 induced respiratory depression: our current understanding. *Journal of Neurophysiology*
538 **125**, 1899–1919 (2021).

539 2. S. D. Comer, C. M. Cahill, Fentanyl: Receptor pharmacology, abuse potential, and
540 implications for treatment. *Neuroscience & Biobehavioral Reviews* **106**, 49–57 (2019).

541 3. C. L. Mattson, Trends and Geographic Patterns in Drug and Synthetic Opioid Overdose
542 Deaths — United States, 2013–2019. *MMWR Morb Mortal Wkly Rep* **70** (2021).

543 4. S. Parida, J. P. De Aquino, M. Sofuoglu, High potency synthetic opioids: Curbing the third
544 wave of the opioid crisis. *Neuroscience & Biobehavioral Reviews* **106**, 9–10 (2019).

545 5. N. Wilson, M. Kariisa, P. Seth, H. Smith, N. L. Davis, Drug and Opioid-Involved Overdose
546 Deaths — United States, 2017–2018. *MMWR Morb Mortal Wkly Rep* **69**, 290–297 (2020).

547 6. A. Mansour, C. A. Fox, S. Burke, F. Meng, R. C. Thompson, H. Akil, S. J. Watson, Mu,
548 delta, and kappa opioid receptor mRNA expression in the rat CNS: An in situ hybridization
549 study. *Journal of Comparative Neurology* **350**, 412–438 (1994).

550 7. J. Zhuang, X. Gao, F. Gao, F. Xu, Mu-opioid receptors in the caudomedial NTS are critical
551 for respiratory responses to stimulation of bronchopulmonary C-fibers and carotid body in
552 conscious rats. *Respir Physiol Neurobiol* **235**, 71–78 (2017).

553 8. R. Hill, R. Santhakumar, W. Dewey, E. Kelly, G. Henderson, Fentanyl depression of
554 respiration: Comparison with heroin and morphine. *Br J Pharmacol* **177**, 254–265 (2020).

555 9. R. C. N. Marchette, E. R. Carlson, E. V. Frye, L. E. Hastings, J. C. M. Vendruscolo, G.
556 Mejias-Torres, S. J. Lewis, A. Hampson, N. D. Volkow, L. F. Vendruscolo, G. F. Koob,
557 Heroin- and Fentanyl-Induced Respiratory Depression in a Rat Plethysmography Model:
558 Potency, Tolerance, and Sex Differences. *J Pharmacol Exp Ther* **385**, 117–134 (2023).

559 10. T. Lewanowitsch, R. J. Irvine, Naloxone and its quaternary derivative, naloxone
560 methiodide, have differing affinities for mu, delta, and kappa opioid receptors in mouse
561 brain homogenates. *Brain Res* **964**, 302–305 (2003).

562 11. N. Fairbairn, P. O. Coffin, A. Y. Walley, Naloxone for heroin, prescription opioid, and illicitly
563 made fentanyl overdoses: Challenges and innovations responding to a dynamic epidemic.
564 *International Journal of Drug Policy* **46**, 172–179 (2017).

565 12. T. Lewanowitsch, R. J. Irvine, Naloxone methiodide reverses opioid-induced respiratory
566 depression and analgesia without withdrawal. *European Journal of Pharmacology* **445**, 61–
567 67 (2002).

568 13. J. T. Lai, C. E. Goldfine, B. P. Chapman, M. M. Taylor, R. K. Rosen, S. P. Carreiro, K. M.
569 Babu, Nobody Wants to Be Narcan'd: A Pilot Qualitative Analysis of Drug Users'
570 Perspectives on Naloxone. *West J Emerg Med* **22**, 339–345 (2021).

571 14. I. Bachmutsky, X. P. Wei, E. Kish, K. Yackle, Opioids depress breathing through two small
572 brainstem sites. *eLife* **9**, e52694 (2020).

573 15. J. T. Bateman, E. S. Levitt, Opioid suppression of an excitatory pontomedullary respiratory
574 circuit by convergent mechanisms. *eLife* **12**, e81119 (2023).

575 16. A. Haji, H. Yamazaki, Y. Ohi, R. Takeda, Distribution of μ receptors in the ventral
576 respiratory group neurons; immunohistochemical and pharmacological studies in
577 decerebrate cats. *Neuroscience Letters* **351**, 37–40 (2003).

578 17. E. S. Levitt, A. P. Abdala, J. F. R. Paton, J. M. Bissonnette, J. T. Williams, μ opioid
579 receptor activation hyperpolarizes respiratory-controlling Kölliker–Fuse neurons and
580 suppresses post-inspiratory drive. *The Journal of Physiology* **593**, 4453–4469 (2015).

581 18. B. Palkovic, V. Marchenko, E. J. Zuperku, E. A. E. Stuth, A. G. Stucke, Multi-Level
582 Regulation of Opioid-Induced Respiratory Depression. *Physiology (Bethesda)* **35**, 391–404
583 (2020).

584 19. G. Montandon, W. Qin, H. Liu, J. Ren, J. J. Greer, R. L. Horner, PreBötzinger Complex
585 Neurokinin-1 Receptor-Expressing Neurons Mediate Opioid-Induced Respiratory
586 Depression. *J. Neurosci.* **31**, 1292–1301 (2011).

587 20. K. T. S. Pattinson, Opioids and the control of respiration. *British Journal of Anaesthesia*
588 **100**, 747–758 (2008).

589 21. M. C. Andresen, D. L. Kunze, Nucleus tractus solitarius--gateway to neural circulatory
590 control. *Annu Rev Physiol* **56**, 93–116 (1994).

591 22. T. L. King, C. M. Heesch, C. G. Clark, D. D. Kline, E. M. Hasser, Hypoxia activates nucleus
592 tractus solitarii neurons projecting to the paraventricular nucleus of the hypothalamus.
593 *American Journal of Physiology-Regulatory, Integrative and Comparative Physiology* **302**,
594 R1219–R1232 (2012).

595 23. L. J. Teppema, J. G. Veening, A. Kranenburg, A. Dahan, A. Berkenbosch, C. Olievier,
596 Expression of c-fos in the rat brainstem after exposure to hypoxia and to normoxic and
597 hyperoxic hypercapnia. *Journal of Comparative Neurology* **388**, 169–190 (1997).

598 24. S. A. Aicher, A. Goldberg, S. Sharma, V. M. Pickel, μ-opioid receptors are present in vagal
599 afferents and their dendritic targets in the medial nucleus tractus solitarius. *Journal of*
600 *Comparative Neurology* **422**, 181–190 (2000).

601 25. A. Disney, K. M. Olson, A. M. Shafer, S. C. Moore, J. P. Anand, J. R. Traynor, S. M.
602 Husbands, Opioid Antagonists from the Orvinol Series as Potential Reversal Agents for
603 Opioid Overdose. *ACS Chem Neurosci* **13**, 3108–3117 (2022).

604 26. E. Solis, K. T. Cameron-Burr, Y. Shaham, E. A. Kiyatkin, Fentanyl-Induced Brain Hypoxia
605 Triggers Brain Hyperglycemia and Biphasic Changes in Brain Temperature.
606 *Neuropsychopharmacol.* **43**, 810–819 (2018).

607 27. S. N. Maletz, B. T. Reid, A. G. Varga, E. S. Levitt, Nucleus Tractus Solitarius Neurons
608 Activated by Hypercapnia and Hypoxia Lack Mu Opioid Receptor Expression. *Front Mol*
609 *Neurosci* **15**, 932189 (2022).

610 28. E. Salas, E. Alonso, M. J. Polanco, M. V. Cano, M. Ruiz-Gayo, L. F. Alguacil, Differential
611 regulation of CDK5 and c-Fos expression by morphine in the brain of Lewis and Fischer
612 344 rat strains. *Neuroscience* **230**, 151–156 (2013).

613 29. P. J. Cabot, P. R. Dodd, T. Cramond, M. T. Smith, Characterization of non-conventional
614 opioid binding sites in rat and human lung. *Eur J Pharmacol* **268**, 247–255 (1994).

615 30. J.-L. Li, T. Kaneko, N. Mizuno, Effects of peripheral nerve ligation on expression of μ-
616 opioid receptor in sensory ganglion neurons: an immunohistochemical study in dorsal root
617 and nodose ganglion neurons of the rat. *Neuroscience Letters* **214**, 91–94 (1996).

618 31. D. Perekopskiy, A. Afzal, S. N. Jackson, L. Muller, A. S. Woods, E. A. Kiyatkin, The Role of
619 Peripheral Opioid Receptors in Triggering Heroin-induced Brain Hypoxia. *Sci Rep* **10**, 833
620 (2020).

621 32. F. Henderson Jr, W. J. May, R. B. Gruber, A. P. Young, L. A. Palmer, B. Gaston, S. J.
622 Lewis, Low-dose morphine elicits ventilatory excitant and depressant responses in
623 conscious rats: Role of peripheral μ-opioid receptors. *Open Journal of Molecular and*
624 *Integrative Physiology* **3**, 111–124 (2014).

625 33. T. L. King, B. C. Ruyle, D. D. Kline, C. M. Heesch, E. M. Hasser, Catecholaminergic
626 neurons projecting to the paraventricular nucleus of the hypothalamus are essential for
627 cardiorespiratory adjustments to hypoxia. *Am J Physiol Regul Integr Comp Physiol* **309**,
628 R721-731 (2015).

629 34. S. McGaraughty, P. Honore, C. T. Wismer, J. Mikusa, C. Z. Zhu, H. A. McDonald, B.
630 Bianchi, C. R. Faltynek, M. F. Jarvis, Endogenous opioid mechanisms partially mediate
631 P2X3/P2X2/3-related antinociception in rat models of inflammatory and chemogenic pain
632 but not neuropathic pain. *Br J Pharmacol* **146**, 180–188 (2005).

633 35. J. T. Bateman, S. E. Saunders, E. S. Levitt, Understanding and countering opioid-induced
634 respiratory depression. *British Journal of Pharmacology* **n/a** (2021).

635 36. J. Neale, J. Strang, Naloxone—does over-antagonism matter? Evidence of iatrogenic harm
636 after emergency treatment of heroin/opioid overdose. *Addiction* **110**, 1644–1652 (2015).

637 37. M. J. Katovich, J. W. Simpkins, J. O'Meara, Effects of opiod antagonists and their
638 quaternary analogs on temperature changes in morphine-dependent rats. *Life Sciences*
639 **39**, 1845–1854 (1986).

640 38. V. Spahn, G. Del Vecchio, D. Labuz, A. Rodriguez-Gaztelumendi, N. Massaly, J. Temp, V.
641 Durmaz, P. Sabri, M. Reidelbach, H. Machelska, M. Weber, C. Stein, A nontoxic pain killer
642 designed by modeling of pathological receptor conformations. *Science* **355**, 966–969
643 (2017).

644 39. J. H. Peters, S. J. McDougall, D. Mendelowitz, D. R. Koop, M. C. Andresen, Isoflurane
645 Differentially Modulates Inhibitory and Excitatory Synaptic Transmission to the Solitary
646 Tract Nucleus. *Anesthesiology* **108**, 675–683 (2008).

647 40. Y. Hu, J. T. Qi, Z. Zhang, M. Q. Luo, Y. W. Wang, Comparative Brain-Wide Mapping of
648 Isoflurane and Ketamine-Activated Nuclei and Functional Networks. *eLife* **12** (2023).

649 41. S. Nomura, Y.-Q. Ding, T. Kaneko, J.-L. Li, N. Mizuno, Localization of μ-opioid receptor-
650 like immunoreactivity in the central components of the vagus nerve: A light and electron
651 microscope study in the rat. *Neuroscience* **73**, 277–286 (1996).

652 42. Z. Zhang, C. Zhang, M. Zhou, F. Xu, Activation of Opioid μ-Receptors, but not δ- or κ-
653 Receptors, Switches Pulmonary C-Fiber-Mediated Rapid Shallow Breathing into An Apnea
654 in Anesthetized Rats. *Respir Physiol Neurobiol* **183**, 211–217 (2012).

655 43. W. T. Talman, M. H. Perrone, D. J. Reis, Evidence for L-glutamate as the neurotransmitter
656 of baroreceptor afferent nerve fibers. *Science* **209**, 813–815 (1980).

657 44. R. J. Cui, B. L. Roberts, H. Zhao, M. C. Andresen, S. M. Appleyard, Opioids inhibit visceral
658 afferent activation of catecholamine neurons in the solitary tract nucleus. *Neuroscience*
659 **222**, 181–190 (2012).

660 45. H. Rhim, R. J. Miller, Opioid receptors modulate diverse types of calcium channels in the
661 nucleus tractus solitarius of the rat. *J. Neurosci.* **14**, 7608–7615 (1994).

662 46. H. Higashi, P. Shinnick-Gallagher, J. P. Gallagher, Morphine enhances and depresses
663 Ca2+-dependent responses in visceral primary afferent neurons. *Brain Research* **251**,
664 186–191 (1982).

665 47. T. W. Bailey, S. M. Appleyard, Y.-H. Jin, M. C. Andresen, Organization and properties of
666 GABAergic neurons in solitary tract nucleus (NTS). *J Neurophysiol* **99**, 1712–1722 (2008).

667 48. A. J. Boxwell, Y. Yanagawa, S. P. Travers, J. B. Travers, The μ-opioid receptor agonist
668 DAMGO presynaptically suppresses solitary tract-evoked input to neurons in the rostral
669 solitary nucleus. *J Neurophysiol* **109**, 2815–2826 (2013).

670 49. N. R. Glatzer, B. N. Smith, Modulation of synaptic transmission in the rat nucleus of the
671 solitary tract by endomorphin-1. *J Neurophysiol* **93**, 2530–2540 (2005).

672 50. S. M. Appleyard, D. Marks, K. Kobayashi, H. Okano, M. J. Low, M. C. Andresen, Visceral
673 afferents directly activate catecholamine neurons in the solitary tract nucleus. *J Neurosci*
674 **27**, 13292–13302 (2007).

675 51. C. S. Bathina, A. Rajulapati, M. Franzke, K. Yamamoto, J. T. Cunningham, S. Mifflin,
676 Knockdown of tyrosine hydroxylase in the nucleus of the solitary tract reduces elevated
677 blood pressure during chronic intermittent hypoxia. *Am J Physiol Regul Integr Comp*
678 *Physiol* **305**, R1031–R1039 (2013).

679 52. E. Floettmann, K. Bui, M. Sostek, K. Payza, M. Eldon, Pharmacologic Profile of Naloxegol,
680 a Peripherally Acting μ-Opioid Receptor Antagonist, for the Treatment of Opioid-Induced
681 Constipation. *J Pharmacol Exp Ther* **361**, 280–291 (2017).

682 53. J. V. Pergolizzi, P. J. Christo, J. A. LeQuang, P. Magnusson, The Use of Peripheral μ-
683 Opioid Receptor Antagonists (PAMORA) in the Management of Opioid-Induced
684 Constipation: An Update on Their Efficacy and Safety. *Drug Des Devel Ther* **14**, 1009–
685 1025 (2020).

686 54. T. M. Tzschentke, Measuring reward with the conditioned place preference (CPP)
687 paradigm: update of the last decade. *Addict Biol* **12**, 227–462 (2007).

688 55. B. C. Ruyle, D. Martinez, C. M. Heesch, D. D. Kline, E. M. Hasser, The PVN enhances
689 cardiorespiratory responses to acute hypoxia via input to the nTS. *Am J Physiol Regul*
690 *Integr Comp Physiol* **317**, R818–R833 (2019).

691

692 Acknowledgements

693 We wish to thank Justin Meyer for breeding the rat colonies that were used in these
694 experiments and for general assistance throughout the experiments. We also thank Mike
695 Cameron (Scripps Institute) for mass spectrometry experiments used for all biodistribution
696 experiments. We also wish to thank Kristine Yoon and Thomas Schodl for their technical
697 assistance.

698 Author Contributions

699 Conceptualization: BCR NM and JAM

700 Methodology: BCR, NM and JAM

701 Formal analysis of all data: BCR, SM, RK, MT and JAH

702 Photometry acquisition and extraction: BCR and JAH

703 Respiratory depression experiments: BCR, SM, RK, MT, JM, SAL

704 Conditioned Place Aversion: BCR, SM, MT, JM

705 Biodistribution experiments: BCR and TL

706 Immunohistochemistry, microscopy and cell counting: BCR, SM, RK, MT, JM, SAL

707 Catheterization surgeries: BCR, SM, RK, MT, JM, SAL

708 Writing of original draft: BCR

709 Writing (review and editing): BCR, RK, JM, SAL, TL, JAH, NM, JAM

710 Funding Acquisition, BR, JM

711 Resources: JM

712 Supervision: BR and JM

Data Availability Statement

The authors confirm that all relevant data are included in the paper and its Supplementary Information files. All data generated in this study are provided in the Supplementary Information/Source Data file. Further information and requests for resources and reagents should be directed to and will be fulfilled by the Lead Contact, Jose A. Morón (jmoron-concepcion @wustl.edu).

Competing Interests

We have no competing interests to declare.

Funding:

National Institute of Health grant R01DA042499 (JMC)

National Institute of Health grant R01DA045463 (JMC)

National Institute of Health grant R01DA054900(JMC)

National Institute of Health grant R56DA059067 (JMC)

Washington University McDonnell Small Grants Program GF0012452 (BCR)

National Institute of Health grant T32DA007261 (BCR)

National Institute of Health grant S10OD030332-01(Michael Cameron, Scripps Research)

FIGURES

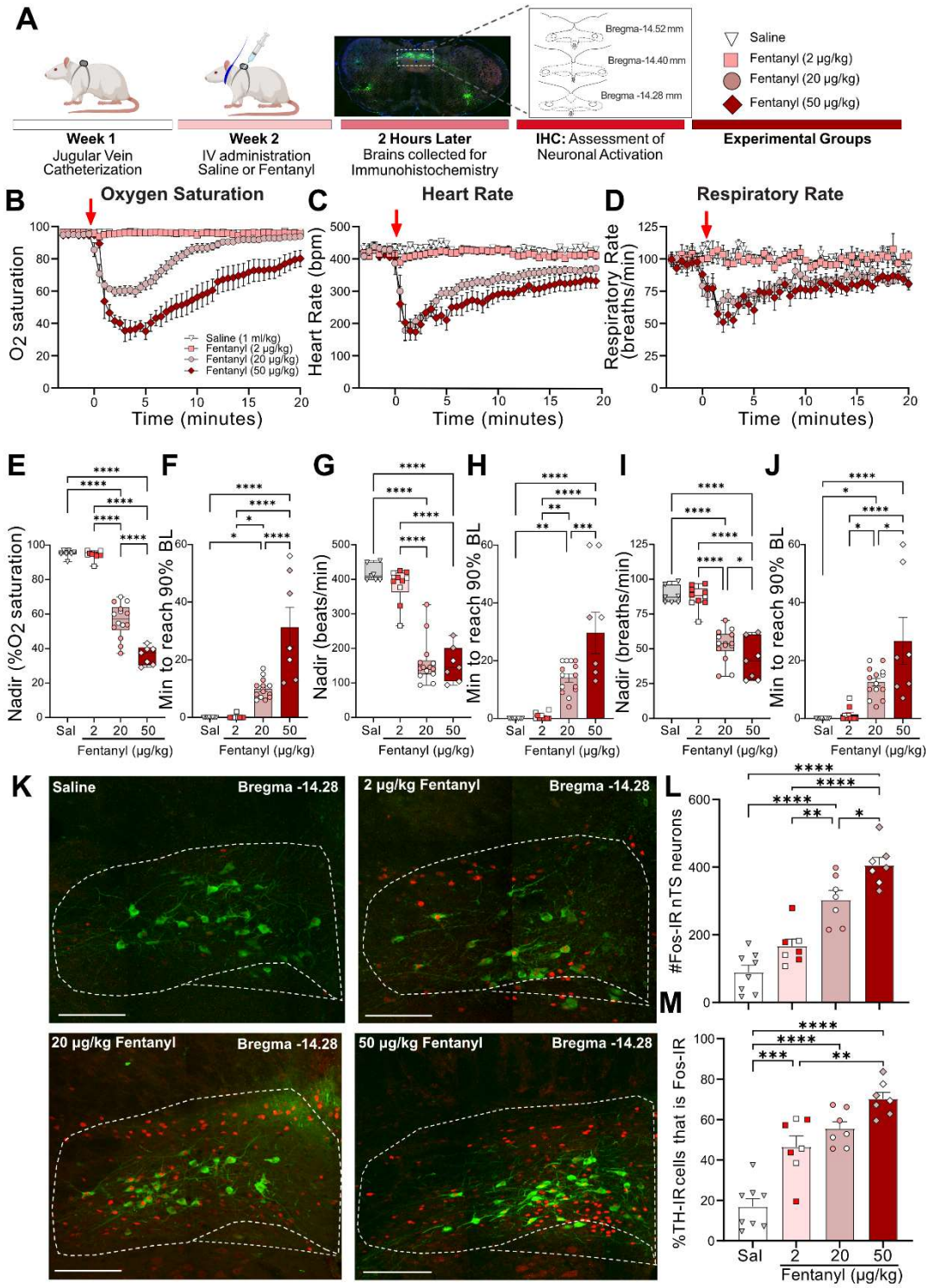
A
Bregma-14.52 mm
Bregma-14.40 mm
Bregma -14.28 mm
Saline
Fentanyl (2 µg/kg)
Fentanyl (20 µg/kg)
Fentanyl (50 µg/kg)
Week 1
Jugular Vein Catheterization
Week 2
IV administration Saline or Fentanyl
2 Hours Later
Brains collected for Immunohistochemistry
IHC: Assessment of Neuronal Activation
Experimental Groups
B
Oxygen Saturation
O2 saturation
Time (minutes)
Saline (1 ml/kg)
Fentanyl (2 µg/kg)
Fentanyl (20 µg/kg)
Fentanyl (50 µg/kg)
C
Heart Rate
Heart Rate (bpm)
Time (minutes)
D
Respiratory Rate
Respiratory Rate (breaths/min)
Time (minutes)
E
Nadir (%O2 saturation)
F
Min to reach 90% BL
G
Nadir (beats/min)
H
Min to reach 90% BL
I
Nadir (breaths/min)
J
Min to reach 90% BL
Sal
2
20
50
Fentanyl (µg/kg)
K
Saline
Bregma -14.28
2 µg/kg Fentanyl
Bregma -14.28
20 µg/kg Fentanyl
Bregma -14.28
50 µg/kg Fentanyl
Bregma -14.28
L
#Fos-IR nTS neurons
M
%TH-IR cells that is Fos-IR
Sal
2
20
50
Fentanyl (µg/kg)

731 **Figure 1: Fentanyl Induces Cardiorespiratory Depression and nTS neuronal activation in**
732 **a dose-dependent manner**
733 **A.** Schematic showing the timeline for OIRD collar experiments. Male and Female SD rats
734 received jugular catheterization surgery. The following week, conscious rats in their home cage
735 received intravenous administration of either saline (n=7, triangles) or fentanyl (2 µg/kg: (n=10,
736 squares); 20 µg/kg, (n=13, circles); 50 µg/kg, (n=7, diamonds). Cardiorespiratory parameters
737 were measured for 3 minutes prior to IV administration and up to 60 minutes after saline or
738 fentanyl. At the conclusion of the experiment, brains were collected from a subset of animals in
739 each group and processed for Fos- and TH- immunoreactivity. Time course data showing
740 oxygen saturation (**B**), heart rate (**C**) and respiratory rate (**D**) data measurements collected in all
741 groups before and after saline or fentanyl. Changes in oxygen saturation were assessed as
742 nadir (lowest value; **E,G,I**) and time to recover to 90% of baseline (pre-saline/fentanyl; **F,H,J**)
743 administration. There was a dose-dependent decrease in the nadir for oxygen saturation (One-
744 way ANOVA, $F_{(3,34)} = 157.4$, $p < 0.0001$; Tukey's post-hoc ****p<0.0001), heart rate (One-way
745 ANOVA $F_{(3, 34)} = 64.96$, $p < 0.0001$; Tukey's post-hoc ****p<0.0001) and respiratory rate (One-
746 way ANOVA, $F_{(3, 34)} = 43.94$, $p < 0.0001$; Tukey's post-hoc ****p<0.0001; *p<0.05). Time to
747 recover to 90% baseline Oxygen Saturation (One-way ANOVA, $F_{(3, 34)} = 25.16$, $p < 0.0001$;
748 Tukey's post-hoc ****p<0.0001, **p<0.01, *p<0.05) heart rate (One-way ANOVA, $F_{(3, 34)} = 23.75$,
749 $p < 0.0001$; Tukey's post-hoc ****p<0.0001, ***p<0.001 **p<0.01) and respiratory rate (One-way
750 ANOVA, $F_{(3, 34)} = 12.61$, $p<0.0001$; Tukey's post-hoc ****p<0.0001, *p<0.05). **K.** Merged
751 photomicrographs of a coronal brainstem section showing representative Fos- and TH-
752 immunoreactivity in the nTS of rats that received intravenous saline or fentanyl. Scale bar = 200
753 µm. **L.** Mean data show that 20 and 50 µg/kg fentanyl induced a significantly greater number of
754 Fos-IR cells in the nTS compared to saline and 2 µg/kg fentanyl. (One-way ANOVA, $F_{(3,25)} =$
755 37.87, $p < 0.0001$; Tukey's post hoc ****p<0.0001, **p<0.001, *p<0.05) **M.** Mean data showing
756 the percentage of TH-IR nTS neurons that displayed Fos-IR. Rats that were given 2 µg/kg
757 fentanyl displayed a significantly higher increase in activated TH-IR neurons compared to
758 saline-treated rats. 50 µg/kg fentanyl induced a significantly higher percentage of activation in
759 TH cells compared to all other groups. (One-way ANOVA, $F_{(3,25)} = 30.99$, $p < 0.0001$; Tukey's
760 post-hoc ****p<0.0001, ***p<0.001; **p<0.01)

761

762

763

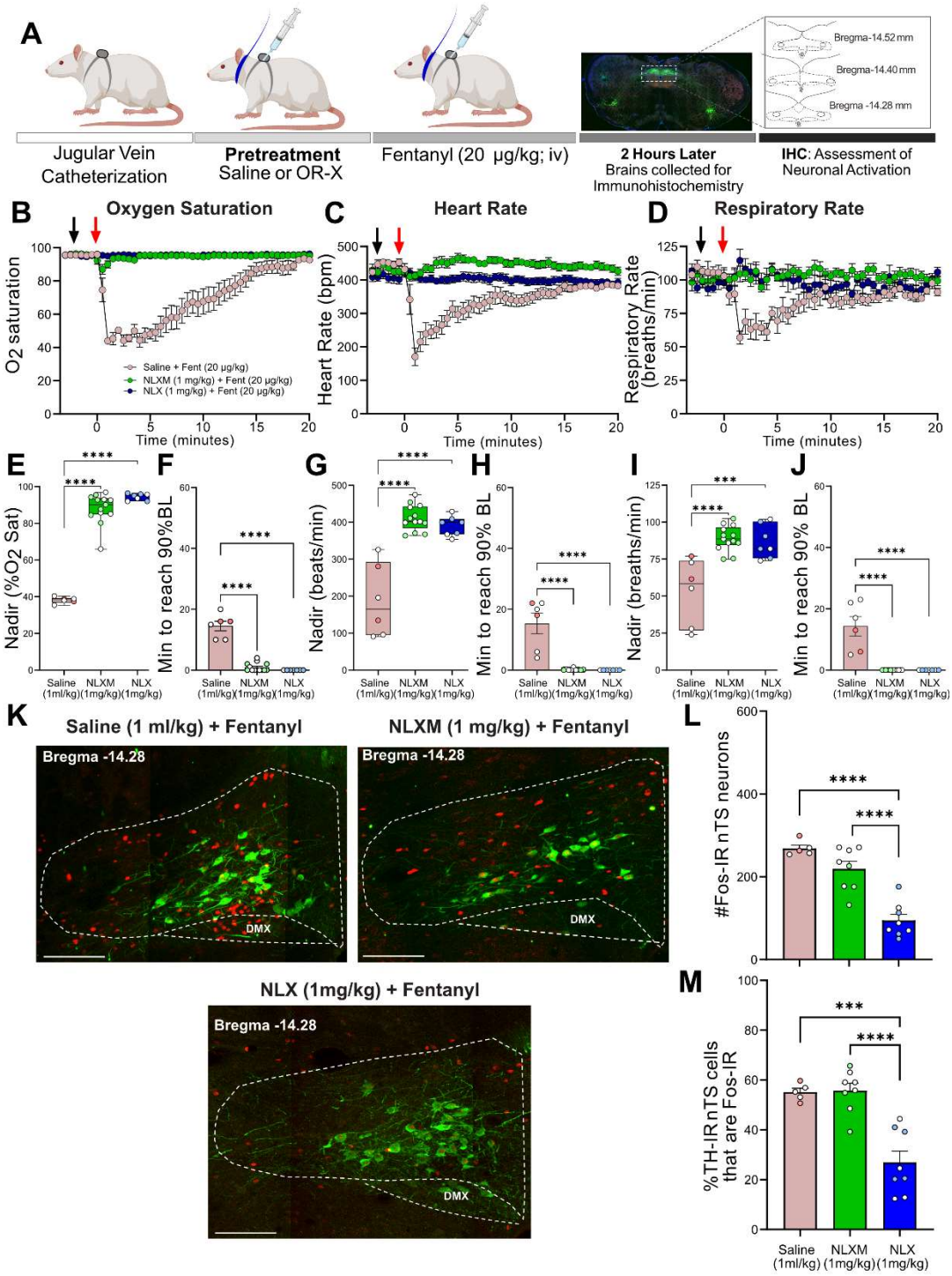

764

765

766

767

768

769 **Figure 2. NLXM Attenuates Respiratory Depression and Limits nTS Neuronal Activation**
770 **Induced by 20 µg/kg Fentanyl: A.** Schematic showing the timeline for OIRD collar
771 experiments. Male and Female SD rats received jugular catheterization surgery. The following
772 week, conscious rats in their home cage received intravenous administration (pretreatment) of
773 either saline (1 ml/kg; n=6), NLX (1 mg/kg; n=7) or NLXM (1 mg/kg; n=13). Two minutes later,
774 all rats received intravenous fentanyl (20 µg/kg). Cardiorespiratory parameters were measured
775 up to 60 minutes fentanyl. At the conclusion of the experiment, brains were collected from a
776 subset of animals in each group and processed for Fos- and TH- immunoreactivity. Time course
777 data showing oxygen saturation (**B**), heart rate (**C**) and respiratory rate (**D**) data measurements
778 collected in all groups before and after saline/OR-X pretreatment and after fentanyl. Changes in
779 oxygen saturation were assessed as nadir (lowest value; **E,G,I**) and time to recover to 90% of
780 baseline (pre-saline/OR-X; **F,H,J**) administration. Mean nadir values were assessed in saline-
781 NLX- and NLXM-pretreated rats (Oxygen Saturation: One-way ANOVA, $F_{(2,23)} = 171.7$, p
782 <0.0001;Tukey's post-hoc test, **** p<0.0001; Heart Rate: One-way ANOVA, $F_{(2,23)} = 37.43$, p
783 <0.0001;Tukey's post-hoc test, **** p<0.0001; Respiratory Rate: One-way ANOVA, $F_{(2,23)} =$
784 15.93, p <0.0001;Tukey's post-hoc test, ****p<0.0001, ***p<0.05). Time to reach 90% baseline
785 in saline-, NLX- and NLXM-pretreated rats. Mean time to reach 90% baseline was assessed for
786 all parameters. Oxygen Saturation: (One-way ANOVA, $F_{(2,23)} = 104.6$, p <0.0001; Tukey's post-
787 hoc test ****p<0.0001; Heart rate: (One-way ANOVA, $F_{(2,23)} = 32.47$, p <0.0001; Tukey's post-
788 hoc test ****p<0.0001); Respiratory rate: (One-way ANOVA, $F_{(2,23)} = 36.43$, p <0.0001; Tukey's
789 post-hoc test). **K.** Merged photomicrographs of a coronal brainstem section showing
790 representative Fos- and TH- immunoreactivity in the nTS of rats that received fentanyl with or
791 without saline or NLX/NLXM pretreatment. Scale bar = 200 µm. Fos-IR and the percentage of
792 TH-IR neurons expressing Fos-IR was evaluated in 3 nTS sections per rat. **L.** Mean data show
793 no significant difference in the number of Fos-IR cells between saline- and NLXM-pretreated
794 rats. NLX-pretreated rats displayed the lowest degree of Fos-IR in the nTS. Number Fos-IR
795 cells: One-way ANOVA, $F_{(2,18)} = 30.52$, p <0.0001; Tukey's post-hoc p<0.0001. **M.** Mean data of
796 the percentage of TH-IR cells expressing Fos-IR. The percentage of Fos-IR TH-IR cells was
797 similar between saline- and NLXM-pretreated rats. NLX-pretreated rats displayed the lowest
798 percentage of Fos-IR in TH-IR cells. Fos+TH/TH: (One-way ANOVA, $F_{(2,18)} = 21.33$, p <0.0001;
799 Tukey's post-hoc **** p<0.0001; *** p<0.05).

800

801

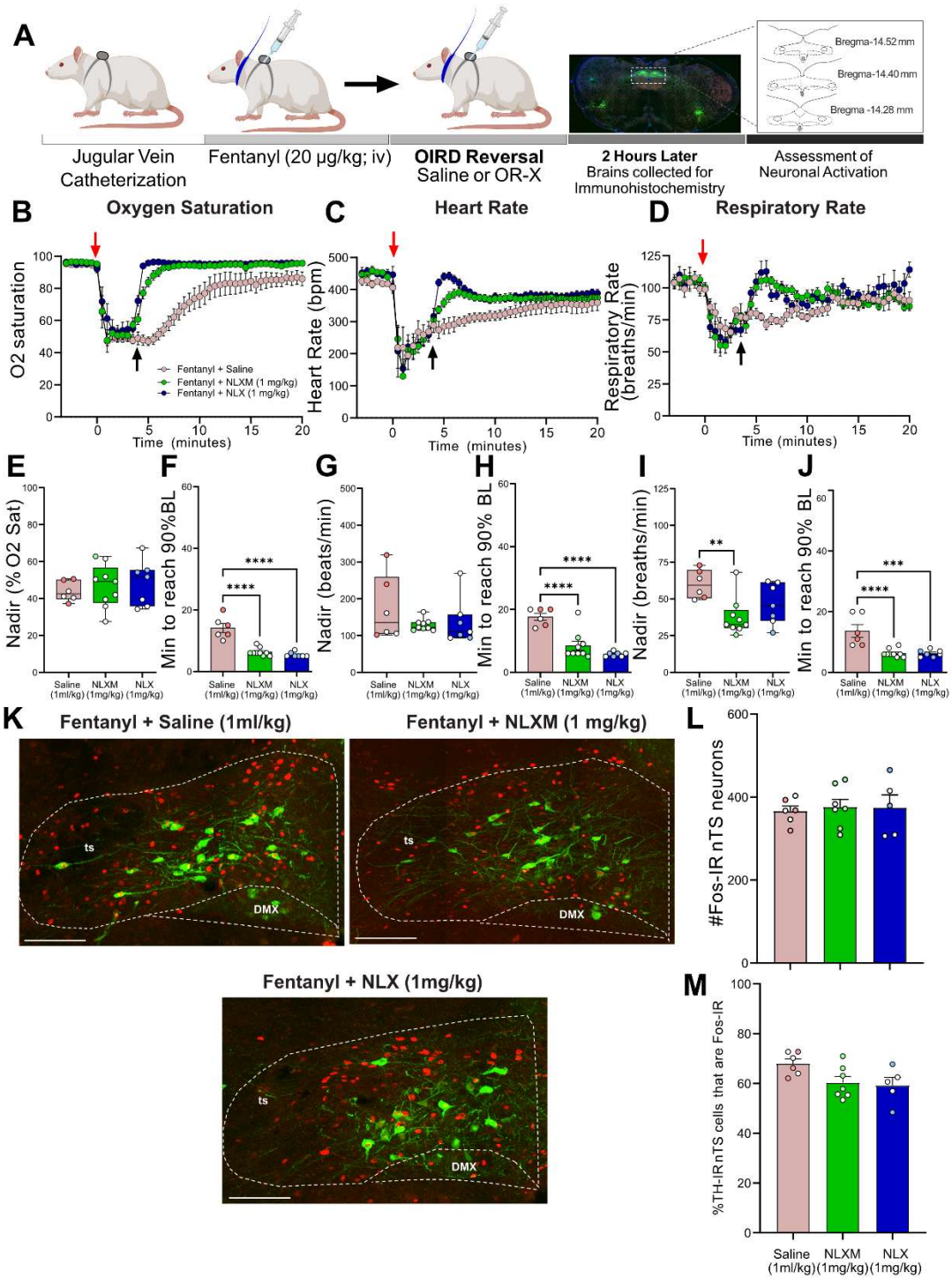
A
Jugular Vein Catheterization
Fentanyl (20 µg/kg; iv)
OIRD Reversal
Saline or OR-X
2 Hours Later
Brains collected for Immunohistochemistry
Assessment of Neuronal Activation
Bregma-14.52 mm
Bregma-14.40 mm
Bregma -14.28 mm
B Oxygen Saturation
C Heart Rate
D Respiratory Rate
O2 saturation
Heart Rate (bpm)
Respiratory Rate (breaths/min)
Time (minutes)
Fentanyl + Saline
Fentanyl + NLXM (1 mg/kg)
Fentanyl + NLX (1 mg/kg)
E
F
G
H
I
J
Nadir (% O2 Sat)
Min to reach 90%BL
Nadir (beats/min)
Nadir (breaths/min)
Saline (1ml/kg)
NLXM (1mg/kg)
NLX (1mg/kg)
K
Fentanyl + Saline (1ml/kg)
Fentanyl + NLXM (1 mg/kg)
Fentanyl + NLX (1mg/kg)
ts
DMX
L
#Fos-IR nTS neurons
M
%TH-IR nTS cells that are Fos-IR

805 **Figure 3 NLXM Reversal of 20 µg/kg Fentanyl-Induced Respiratory Depression is**
806 **Comparable to NLX. A.** Schematic showing the timeline for OIRD reversal experiments. Male
807 and Female SD rats received jugular catheterization surgery. The following week, conscious
808 rats in their home cage received intravenous fentanyl (20 µg/kg). Four minutes later, rats
809 received intravenous administration (reversal) of either saline (1 ml/kg; n=6), NLX (1 mg/kg;
810 n=7) or NLXM (1 mg/kg; n=9). Cardiorespiratory parameters were measured up to 60 minutes
811 after fentanyl. At the conclusion of the experiment, brains were collected from a subset of
812 animals in each group and processed for Fos- and TH- immunoreactivity. Time course data
813 showing oxygen saturation (**B**), heart rate (**C**) and respiratory rate (**D**) data measurements
814 collected in all groups before and after fentanyl and saline/OR-X administration. Changes in
815 oxygen saturation were assessed as nadir (lowest value; **E,G,I**) and time to recover to 90% of
816 baseline (pre-saline/OR-X; **F,H,J**) administration. Mean nadir values were assessed in saline-
817 NLX- and NLXM-pretreated rats (Oxygen Saturation: One-way ANOVA, $F_{(2,19)} = 0.2854$,
818 p=0.7549; Heart Rate: One-way ANOVA, $F_{(2,19)} = 1.076$, p=0.3609; Respiratory Rate: One-way
819 ANOVA, $F_{(2,19)} = 5.823$, p=0.0107. Time to reach 90% baseline in saline-, NLX- and NLXM-
820 pretreated rats. Mean time to reach 90% baseline was assessed for all parameters. Oxygen
821 Saturation: One-way ANOVA, $F_{(2,19)} = 34.38$, p <0.0001;Tukey's post-hoc test, **** p<0.0001;
822 Heart Rate: One-way ANOVA, $F_{(2,19)} = 24.50$, p <0.0001;Tukey's post-hoc test, **** p<0.0001;
823 Respiratory Rate: One-way ANOVA, $F_{(2,19)} = 14.68$, p=0.0001;Tukey's post-hoc test, ***p<0.05).
824 **K.** Merged photomicrographs of a coronal brainstem section showing representative Fos- and
825 TH- immunoreactivity in the nTS of rats that received fentanyl followed by saline or NLX/NLXM.
826 Scale bar = 200 µm. **L.** Mean data of the number of Fos-IR cells evaluated in 3 nTS sections
827 per rat Number Fos-IR cells: One-way ANOVA, $F_{(2,15)} = 0.07269$, p=0.9302. **M.** Mean data of the
828 percentage of TH-IR cells that expressing Fos-IR: One-way ANOVA, $F_{(2,16)} = 3.507$, p=0.0563.
829 There were no significant differences in the number of Fos-IR cells or the percentage of TH-IR
830 cells expressing Fos-IR between groups.
831

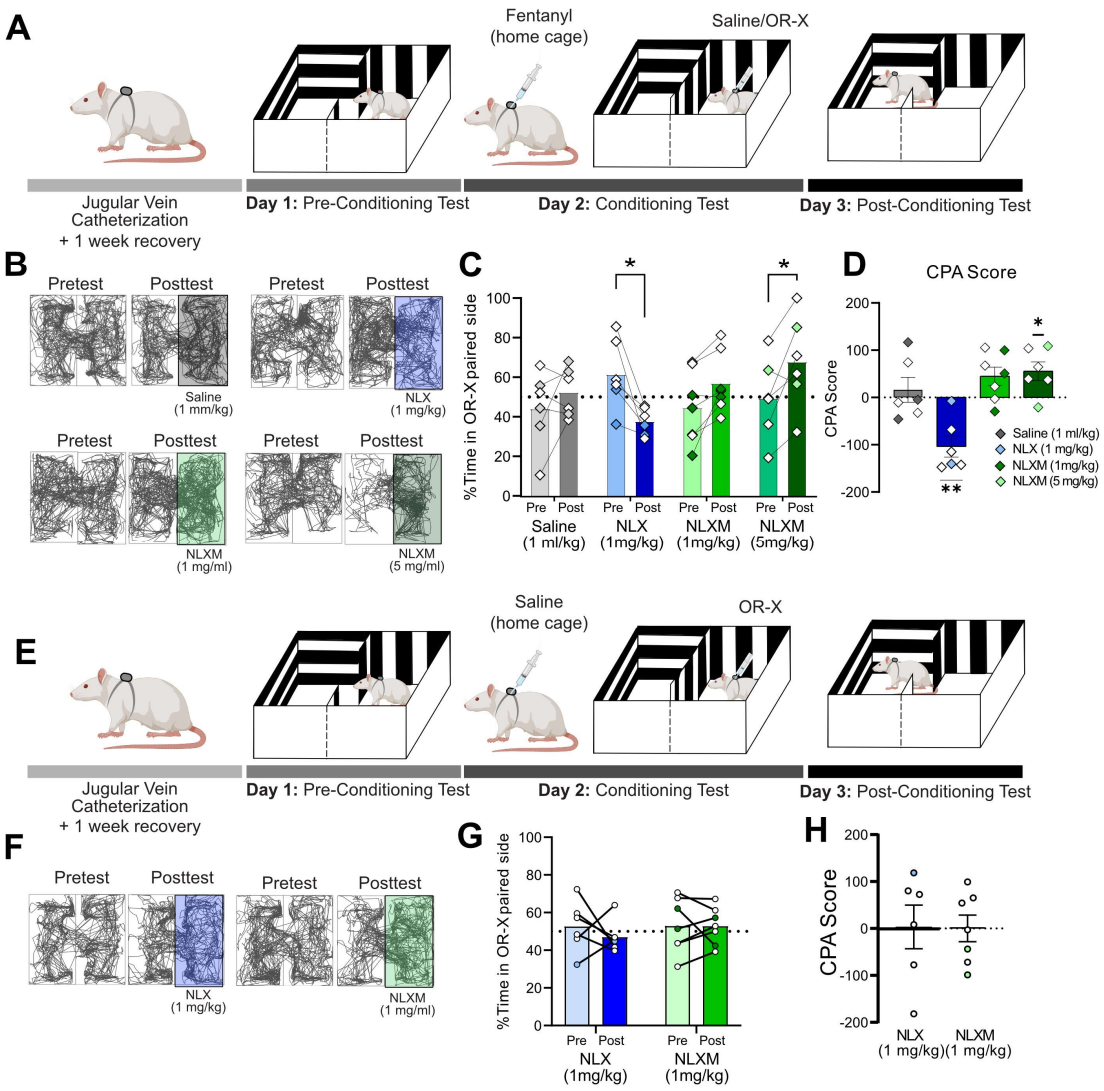
A
Fentanyl
(home cage)
Saline/OR-X
Jugular Vein
Catheterization
+ 1 week recovery
Day 1: Pre-Conditioning Test
Day 2: Conditioning Test
Day 3: Post-Conditioning Test
B
Pretest
Posttest
Saline
(1 mm/kg)
NLX
(1 mg/kg)
NLXM
(1 mg/ml)
NLXM
(5 mg/ml)
C
% Time in OR-X paired side
Pre
Post
Saline
(1 ml/kg)
NLX
(1mg/kg)
NLXM
(1mg/kg)
NLXM
(5mg/kg)
D
CPA Score
Saline (1 ml/kg)
NLX (1 mg/kg)
NLXM (1mg/kg)
NLXM (5 mg/kg)
E
Saline
(home cage)
OR-X
Jugular Vein
Catheterization
+ 1 week recovery
Day 1: Pre-Conditioning Test
Day 2: Conditioning Test
Day 3: Post-Conditioning Test
F
Pretest
Posttest
NLX
(1 mg/kg)
NLXM
(1 mg/ml)
G
% Time in OR-X paired side
Pre
Post
NLX
(1mg/kg)
NLXM
(1mg/kg)
H
CPA Score
NLX
(1 mg/kg)
NLXM
(1 mg/kg)

841 **Figure 4: NLXM reversal of OIRD is not aversive. A**. Schematic of the Conditioned Place
842 Aversion (CPA) experimental design for rats given fentanyl followed by saline or OR-X.
843 Catheterized rats underwent a pretest (Day 1). On the test day (Day 2), rats received fentanyl
844 (50 µg/kg) in their home cages. Four minutes later, rats received intravenous saline, NLX or
845 NLXM in the paired side of the box. During the post-test (Day 3), rats were placed in the box
846 and allowed to explore both compartments. **B.** Track plot data showing movement in both sides
847 of the CPA box during the Pre-test (day 1) and Post-test (Day 3). For each condition, the Pre-
848 and Post-test data is from the same animal. In these representative examples, the saline or OR-
849 X paired side is shown on the right side of the box. However, the paired side was balanced
850 between left and right sides of the box for all groups. **C.** Mean data with individual plots showing
851 changes in the time spent on the saline- and OR-X paired side. **D.** The CPA score (calculated
852 as time spent in the saline or OR-X paired compartment during posttest minus the time spent in
853 the same compartment during the pretest. For CPA scores, one-sample t-test from hypothetical
854 value (no aversion). There was a significant decrease in the CPA score for NLX treated rats
855 ($t=3.706$ ($df=4$, $p<0.05$). 1 mg NLXM: $t=2.340$, $df=6$ $p=0.578$; 5 mg/kg NLXM: $t=2.225$, $df=7$,
856 $p=0.0614$. Saline, $t=0.6113$ ($df=5$, $p=0.5677$). **E**. Schematic of the Conditioned Place Aversion
857 (CPA) experimental design for saline-pretreated animals in combination with saline or OR-X. **F.**
858 Track plot data showing movement in both sides of the CPA box during the Pre-test (day 1) and
859 Post-test (Day 3). For each condition, the Pre- and Post-test data is from the same animal. In
860 these representative examples, the saline or OR-X paired side is shown on the right side of the
861 box. However, the paired side was balanced between left and right sides of the box for all
862 groups. **G.** Mean data with individual plots showing changes in the time spent on the saline- and
863 OR-X paired side. There was no significant difference between the time spent in NLX or NLXM
864 paired side in these animals **H.** The CPA score (calculated as time spent in the saline or OR-X
865 paired compartment during posttest minus the time spent in the same compartment during the
866 pretest. For CPA scores, one-sample t-test from hypothetical value (no aversion). There was no
867 significant difference between NLX or NLXM treated animals. NLX: $t=0.2812$, $df=7$, $p=0.7867$.
868 NLXM, $t=0.005032$, $d=6=$. $P=0.9961$.

869

870

871

872

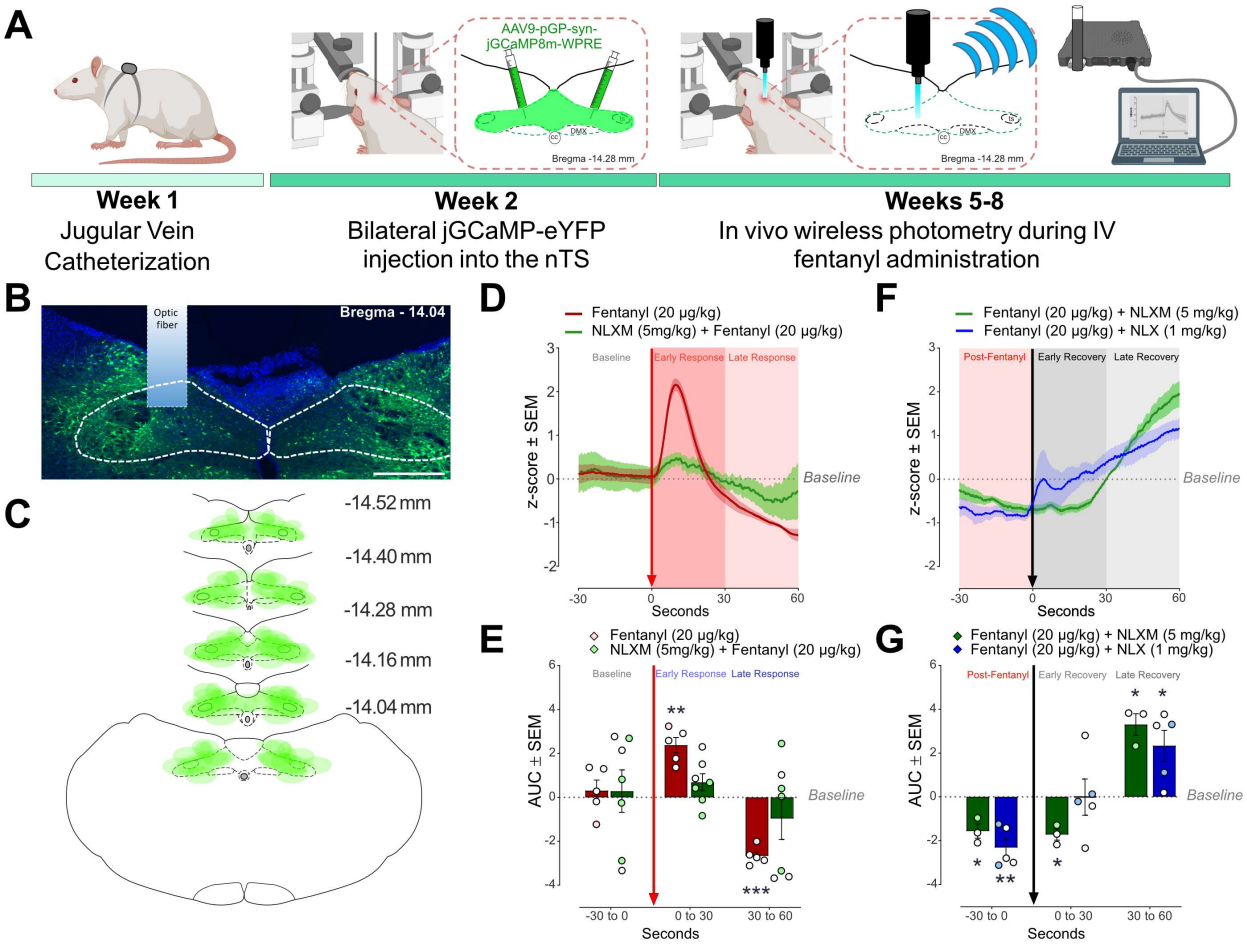
A
AAV9-pGP-syn-jGCaMP8m-WPRE
Bregma -14.28 mm
Week 1
Jugular Vein Catheterization
Week 2
Bilateral jGCaMP-eYFP injection into the nTS
Weeks 5-8
In vivo wireless photometry during IV fentanyl administration
B
Optic fiber
Bregma - 14.04
C
-14.52 mm
-14.40 mm
-14.28 mm
-14.16 mm
-14.04 mm
D
Fentanyl (20 µg/kg)
NLXM (5mg/kg) + Fentanyl (20 µg/kg)
Baseline
Early Response
Late Response
z-score ± SEM
Seconds
E
AUC ± SEM
-30 to 0
0 to 30
30 to 60
F
Fentanyl (20 µg/kg) + NLXM (5 mg/kg)
Fentanyl (20 µg/kg) + NLX (1 mg/kg)
Post-Fentanyl
Early Recovery
Late Recovery
G

884 **FIGURE 5: Fentanyl-induced nTS activity is mediated by peripheral MORs**.
885 **A.** Experimental timeline. Male and female rats underwent jugular catheterization surgery,
886 followed by bilateral nanoinjection of jGCaMP8m into the nTS and then allowed 3-5 weeks for
887 viral expression. On the test day, rats were anesthetized and placed in a stereotax. The nTS
888 was exposed and a fiber was lowered into the nTS. **B.** Representative example of eYFP
889 expression and fiber placement in the nTS. Scale bar = 200 µm. **C.** Spread of overlay of
890 individual animal viral expression across the caudal-rostral extent of the nTS. **D.** nTS cell
891 response (mean z-score) aligned to 20 µg/kg fentanyl administration (red arrow) at Baseline (-
892 30-0 seconds), early response (0-30 seconds) and late response (30-60 seconds) in rats that
893 received 20 µg/kg fentanyl only (red trace) or 5 mg/kg NLXM followed by 20 µg/kg fentanyl
894 (green trace). **E.** Area under the curve (AUC) was calculated during baseline (-30 to 0 seconds),
895 Early Response (0 to 30 seconds) or Late Response (30 to 60 seconds). For AUC graphs, one-
896 sample t-test from hypothetical zero value. In rats that received fentanyl only, there was a
897 significant increase in the AUC during the Early Phase (t=6.747, df=4 ** p=0.0025) followed by a
898 significant decrease in the Late Phase (t=14.35, df=4 *** p=0.0001). In rats that received 5
899 mg/kg NLXM prior to 20 µg/kg fentanyl, no differences in AUC were observed at any time point
900 (Baseline; t=0.2916, df=6 p=0.7804; Early Phase; t=1.760, df=6 p=0.1288; 30-60 seconds;
901 t=1.002, df=6, p=0.3548). **F.** nTS cell response (mean z-score) aligned to MOR antagonists
902 (black arrow). Rats received iv 20 µg/kg fentanyl (Post-Fentanyl phase, -30 to 0 seconds) prior
903 to MOR antagonist infusion of NLX (1 mg/kg, blue trace) or NLXM (5 mg/kg, green trace). Data
904 during Early Recovery (0 to 30 seconds) and Late Recovery (30 to 60 seconds) are shown. **G.**
905 Mean data showing AUC analyses for both groups. For all graphs, one-sample t-test from
906 hypothetical zero value. NLXM-treated rats had a significant decrease in activity from Post-
907 Fentanyl baseline prior to NLXM (t=4.799, df=2 * p=0.0408) and during the Early Recovery
908 phase (t=6.683, df=2 p=0.0217), and exhibited enhanced activity above baseline during the Late
909 Recovery phase (t=6.716, df=2, * p=0.0215). NLX-treated rats displayed a similar decrease
910 below baseline prior to NLX. No difference from baseline was observed during the Early
911 Recovery phase (t=0.01238, df=4 p=0.9907), and a significant increase above baseline was
912 observed during the Late Recovery phase (t=3.318, df=4, * p=0.0215).
913
914
915
916

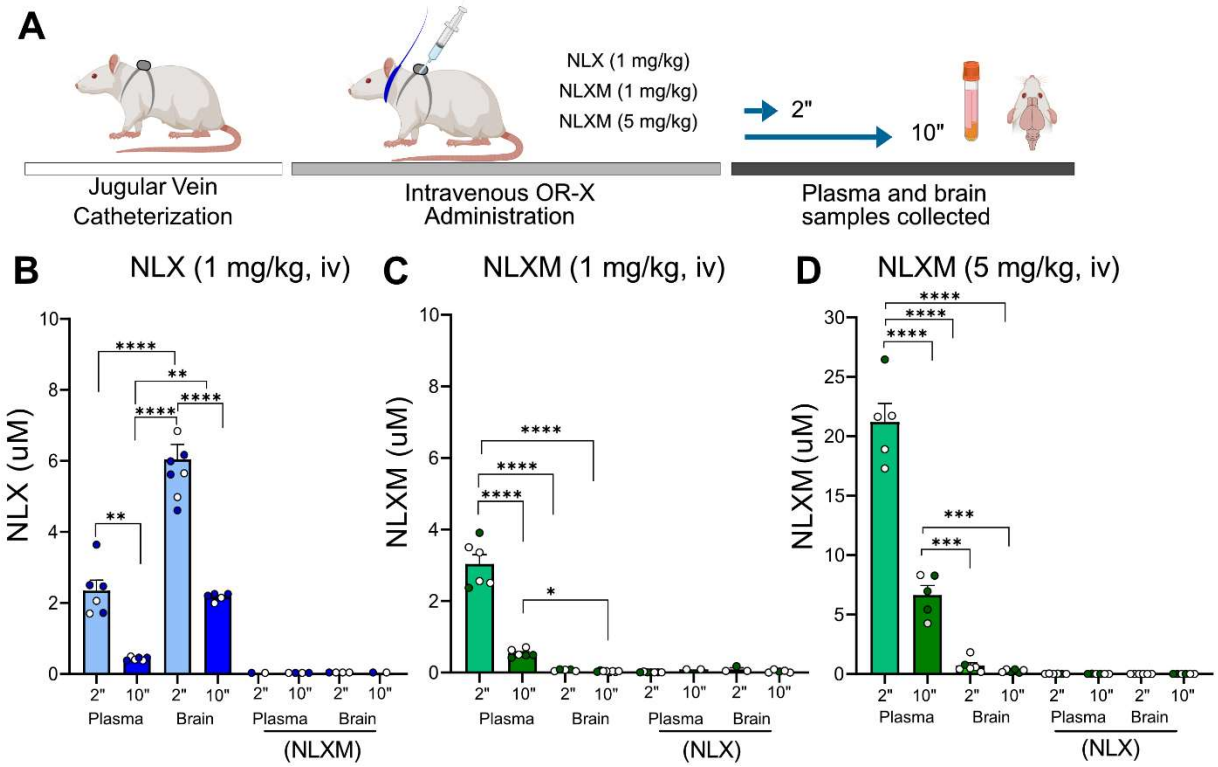
A
NLX (1 mg/kg)
NLXM (1 mg/kg)
NLXM (5 mg/kg)
2"
10"
Jugular Vein Catheterization
Intravenous OR-X Administration
Plasma and brain samples collected
B
NLX (1 mg/kg, iv)
NLX (uM)
C
NLXM (1 mg/kg, iv)
NLXM (uM)
D
NLXM (5 mg/kg, iv)
NLXM (uM)
2" 10" 2" 10" 2" 10" 2" 10"
Plasma Brain Plasma Brain
(NLXM)
(NLX)

923 **Figure 6: NLXM does not cross the blood brain barrier**. **A**. Timeline of Biodistribution
924 experiments. Male and female SD rats received intravenous jugular catheterization surgery. The
925 following week, rats were anesthetized and received intravenous NLX (1 mg/kg) or NLXM (1 or
926 5 mg/kg). Rats were sacrificed 2- and 10- minutes after IV admin. Plasma was extracted from
927 trunk blood and intact brains were removed and rapidly frozen with liquid nitrogen. **B**. Amount of
928 NLX detected in plasma and brain samples at 2 and 10 minutes after intravenous NLX (1
929 mg/kg). One-way ANOVA, $F_{(3,21)} = 66.05$, $p < 0.0001$; Tukey's post-hoc test, **** $p<0.0001$; **
930 $p<0.01$. **C**. Amount of NLXM detected in plasma and brain samples at 2 and 10 minutes after
931 intravenous NLXM (1 mg/kg). One-way ANOVA, $F_{(3,21)} = 125.6$, $p < 0.0001$; Tukey's post-hoc
932 test, **** $p<0.0001$; * $p<0.05$. **D**. Amount of NLXM detected in plasma and brain samples at 2
933 and 10 minutes after intravenous NLXM (5 mg/kg). One-way ANOVA, $F_{(3,18)} = 144.0$, $p < 0.0001$;
934 Tukey's post-hoc test, **** $p<0.0001$; *** $p<0.001$.
935
936
937
938
939
940
941
942
943
944
945
946
947
948
949